AN APPLICATION OF FEEDBACK TO ELECTROMAGNETIC SEISMOMETERS

by

ROBERT DAVID MELDRUM

B.Sc., University of British Columbia, 1963

A THESIS SUBMITTED IN PARTIAL FULFILMENT OF

THE REQUIRMENTS FOR THE DEGREE OF

MASTER OF SCIENCE

in the Department

of

GEOPHYSICS

We accept this thesis as conforming to the

required standard

THE UNIVERSITY OF BRITISH COLUMBIA

October, 1965

In presenting this thesis in partial fulfilment of the requirements for an advanced degree at the University of British Columbia, I agree that the Library shall make it freely available for reference and study. I further agree that permission for extensive copying of this thesis for scholarly purposes may be granted by the Head of my Department or by his representatives. It is understood that copying or publication of this thesis for financial gain shall not be allowed without my written permission.

Department of Geophysics

The University of British Columbia
Vancouver 8, Canada

Date October, 1965

ABSTRACT

Negative feedback can be applied to an electromagnetic seismometer through the coil terminals using a Maxwell impedance bridge to bypass the coil impedance. The application of feedback by this method obviates the need for a second transducer, and permits direct calibration of the feedback seismometer.

Feedback of a simulated ground acceleration proportional to the acceleration of the suspended mass effectively increases the mass, lengthening the natural period of the seismometer. Displacement feedback effectively stiffens the spring, decreasing the resonant period, while the seismometer damping can be increased with velocity feedback.

Experimentally determined sensitivity curves obtained with a Willmore Mk.I seismometer demonstrate the capabilities of negative feedback in altering the response of the seismometer. A resonant period of 17 sec. corresponding to an equivalent suspended mass of 1230 kg. is readily obtained.

A discussion of instrument noise in the feedback seismometer is included.

AN APPLICATION OF FEEDBACK TO ELECTROMAGNETIC SEISMOMETERS

Table of Contents

LIST OF TABLES

LIST OF FIGURES

ACKNOWLEDGEMENTS

The concept of the Maxwell bridge as a means of applying feedback to a seismometer was conceived by Dr. R. D. Russell, who is better known in the field of mass spectrometry than seismology. It was under his very able guidance that this study was conducted. His advice and encouragement are truly appreciated.

Considerable profit was derived from discussions with Oliver Jensen, a fellow graduate student who is extending this research with the construction of an operating seismograph employing a feedback seismometer based on the principles described herein. It is hoped that he too has benefited.

The interest expressed in this project by Peter Michalow, electronics technician in the Geophysics Department, is appreciated. His assistance in overcoming various practical difficulties was invaluable.

The author is grateful to Dr. A. M. Crooker of the U.B.C. Physics Department whose analog computer was used in the experimental work, and to the Observatories Branch of the Department of Mines and Technical Surveys, Ottawa, who generously loaned two Willmore Mk.I seismometers to the Geophysics Department for this and ensuing studies.

Financial assistance was received from National Research Council of Canada research grants to Drs. J. A. Jacobs and R. D. Russell.

Chapter 1 INTRODUCTION TO SEISMOMETRY

1.1 Seismometers and seismographs

The seismograph is an instrument which provides a record of the infinitesimal movements of the ground caused by elastic waves travelling through the earth from distant earthquakes, and from other lesser sources. The detecting unit of the seismograph, the seismometer[1], produces a signal related to the ground motion. This signal, which may be electrical or mechanical (eg. the deflection of a pointer from a zero mark), is then converted by a recording system into a continuous digital or analog record.

The seismometer generally consists of a suspended mass which, because of its inertia, tends to remain at rest while the frame from which it is suspended moves with the ground[2]. Ideally, the apparent motion of the mass is 180° out of phase with the motion of the ground. In practice, however, the suspension system applies a restoring force to the mass proportional to its displacement, with the result that it tends to oscillate with a period determined by the suspended mass and the stiffness of the suspension. It is

---

1. The terms seismograph and seismometer have been differently defined by various authorities. The interpretation given here reflects the opinion of the author and is based on definitions given by J. H. Hodgson [6] and by P. L. Willmore [15].

2. The exception is the strain seismometer, which directly measures the compressions and dilations of the ground as the seismic waves pass.

necessary to apply a damping force, proportional to the velocity of the mass and opposing its motion, to reduce this tendency.

The mass is generally constrained to move in one direction only, and the seismograph records one component of the ground motion. Seismographs have been built however, to produce records of all three components simultaneously.

The detection of the differential motion between the mass and the frame can be accomplished in many ways. The original method involved the magnification of the mass's movements by an intricate system of levers, and the recording of the magnified motion by a stylus writing on smoked paper. This method of recording had several disadvantages including the inconvenience of smoked paper records and the necessity of large suspended masses to overcome the friction between the paper and stylus and in the lever system.

With the use of transducers[3] and electrical recording methods, higher magnifications with smaller masses were achieved. Many seismographs use electromagnetic transducers[4] to drive sensitive galvanometers, the suspension movements of which are optically magnified and recorded on photographic paper.

A great variety of transducer systems and recording methods have been employed in seismographs. Electrostatic

---

3. Devices which convert mechanical energy into electrical energy and vice versa.

4. See Appendix A - Electromagnetic transducer.

transducers in which one plate of a capacitor is attached to the suspended mass are often used in long period seismographs. These transducers allow external power sources and AC amplification methods to be used. Chart recorders allowing the record to be viewed as it is being written, and digital recorders are in use, while magnetic tape recording methods are being developed.

The method of suspending the mass varies considerably between seismometers, and usually depends on the purpose for which the instrument was designed [5,7]. A vertical component seismometer with a simple spring suspension is discussed in the following section.

1.2 Seismometer and seismograph response

Fig.1-1 shows a simple vertical component seismometer consisting of a mass M, suspended by a spring of stiffness U, and damped by a fluid dashpot with damping constant D.

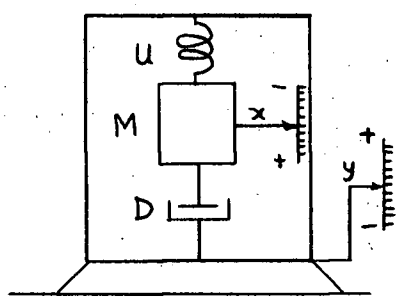

Fig.1-1 Simple seismometer.

If y is the displacement of the ground in space, and x is the displacement of the mass with respect to the case, then the displacement of the mass in space is $(x-y)$ and its acceleration is $\frac{d^2}{dt^2}(x-y)$. The forces acting on the mass due to the spring and dashpot are respectively $-Ux$ and $-D\frac{dx}{dt}$ for displacement x and velocity $\frac{dx}{dt}$ of the mass with respect to the case.

Applying Newton's second law,

$$\frac{M d^2(x-y)}{dt^2} = -Ux - D\frac{dx}{dt}$$

and the equation of motion is

$$M\frac{d^2x}{dt^2} + D\frac{dx}{dt} + Ux = M\frac{d^2y}{dt^2}$$

or

$$\frac{d^2x}{dt^2} + 2\zeta_s\omega_s\frac{dx}{dt} + \omega_s^2 x = \frac{d^2y}{dt^2}$$

where ζ_s is the damping ratio, and ω_s is the angular natural frequency. Since the seismometer satisfies a second order differential equation, it is termed a second order mechanical system.

A Laplace transformation of the equation of motion and rearrangement gives the transfer function of the seismometer,

$$\frac{X(s)}{Y(s)} = \frac{Ms^2}{Ms^2 + Ds + U} = \frac{s^2}{s^2 + 2\zeta_s\omega_s s + \omega_s^2}$$

where the upper case symbols represent the transforms of the lower case quantities[5].

If the ground acceleration is regarded as the input, the transfer function is

$$\frac{X(s)}{\ddot{Y}(s)} = \frac{X(s)}{s^2 Y(s)} = \frac{1}{s^2 + 2\zeta_s\omega_s s + \omega_s^2}$$

The response to a sinusoidal ground acceleration $\ddot{y}_o e^{j\omega t}$ ($\ddot{y}_o$ real) is, by definition of the transfer function $\frac{X(j\omega)}{\ddot{Y}(j\omega)}\ddot{y}_o e^{j\omega t} = x_o e^{j\omega t}$. $\frac{x_o}{\ddot{y}_o} = \frac{X(j\omega)}{\ddot{Y}(j\omega)}$ is the frequency response

---

5. See Appendix B - Laplace transforms and transfer functions.

of the seismometer to sinusoidal ground accelerations and $\left|\frac{X(j\omega)}{\ddot{Y}(j\omega)}\right|$ is the acceleration sensitivity.

The transfer function of an electromagnetic transducer is $\frac{E(s)}{sX(s)} = g$ where g is the transducer constant, and $E(s)$ and $sX(s)$ are the transforms of the output emf and relative velocity of the transducer elements respectively. Therefore, regarding the ground acceleration as the input, the transfer function of a seismometer with an electromagnetic transducer is

$$\frac{E(s)}{\ddot{Y}(s)} = \frac{E(s)}{X(s)} \cdot \frac{X(s)}{\ddot{Y}(s)} = \frac{sg}{s^2 + 2\zeta_s \omega_s s + \omega_s^2}$$

$\left|\frac{E(j\omega)}{\ddot{Y}(j\omega)}\right|$ is then the acceleration sensitivity of the electromagnetic seismometer and is plotted against the period of the ground movement in Fig.1-2. $T_s = \frac{2\pi}{\omega_s}$ is the resonant period of

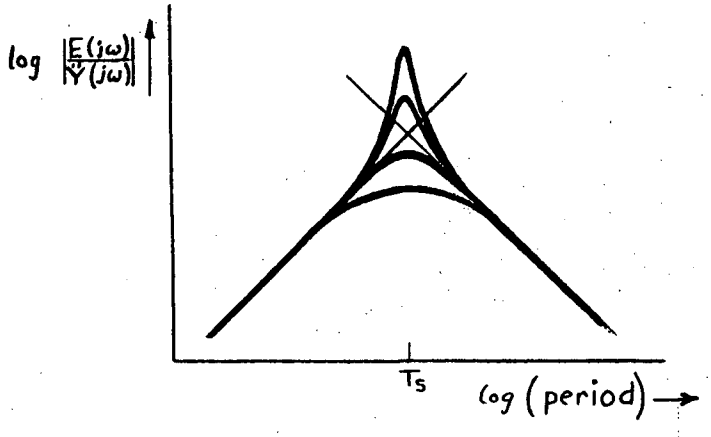

Fig.1-2 Electromagnetic seismometer acceleration sensitivity.

the seismometer.

Now, the transfer function of a galvanometer is

$$\frac{\Theta(s)}{I(s)} = \frac{h}{s^2 + 2\zeta_g \omega_g s + \omega_g^2}$$

where $\Theta(s)$ is the transformed angular deflection of the suspension,

$I(s)$ is the transformed coil current,

ζ_g is the galvanometer damping ratio,

ω_g is the galvanometer angular natural frequency,

h is the galvanometer transducer constant.

If the galvanometer is connected directly to the electromagnetic seismometer, and if the galvanometer reaction (the effect of the movements of the galvanometer suspension on the motion of the suspended mass of the seismometer) and the coil inductances are negligible, the transfer function of the resulting seismograph is

$$\frac{\Theta(s)}{\ddot{Y}(s)} = a \frac{gs}{s^2 + 2\zeta_s\omega_s s + \omega_s^2} \cdot \frac{h}{s^2 + 2\zeta_g\omega_g s + \omega_g^2}$$

where a is an attenuation constant. $\left|\frac{\Theta(j\omega)}{\ddot{Y}(j\omega)}\right|$ is the acceleration sensitivity of the seismograph and is plotted in Fig.1-3. T_g and T_s are the resonant periods of the galvanometer and seismometer respectively.

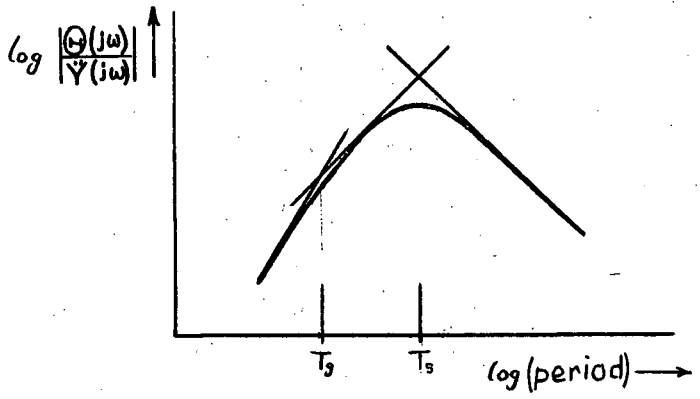

Fig.1-3 Electromagnetic seismograph acceleration sensitivity.

It is seen that the passband of the electromagnetic

seismograph is controlled by the galvanometer on the short period side and by the seismometer on the long period side. If T_g and T_s were interchanged, the response curve would have the same appearance, but a decreased sensitivity would result.

In the past, one of the aims of seismologists in the construction of seismographs was a high sensitivity over as broad a period range as possible. This practice resulted in the discovery of microseisms, a continuous seismic background noise with periods ranging from 1 to 7 seconds. Further increases in sensitivity were possible only in period ranges for which the microseismic noise level was low. This led to the use of two seismographs for each component of ground motion recorded - one recording long period signals, and the other, short periods - with their response curves positioned to exclude the main microseismic region (Fig.1-4).

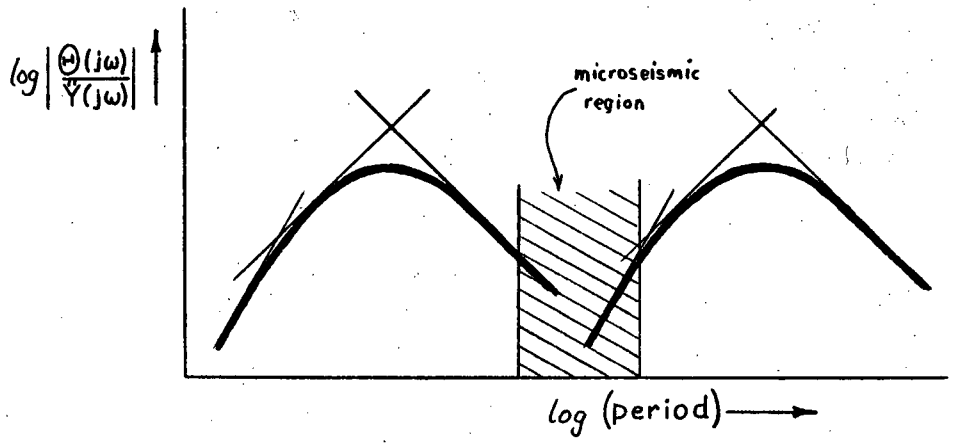

Fig.1-4 Acceleration sensitivities of long and short period seismographs in relation to the microseismic region.

This attitude has changed however, with the possibility of using slow speed magnetic tape recording in seismology. A slow speed tape recorder with flat response combined with a

broadband seismometer would record a wide spectrum of seismic signals. The tapes could later be played back through various filters to obtain the desired results. In this manner, no information is lost through filtering as long as the system is strictly linear.

The bandwidth of a seismograph can be increased by various methods, the simplest being the lengthening of the seismometer period and the shortening of the galvanometer period. Long seismometer periods in vertical instruments require the use of weaker springs which are subject to thermoelastic effects and mechanical fatigue. These effects cause the mass to drift from its equilibrium position, restricting the practical length of periods obtainable by this method.

Willmore [14] has shown that broad-band characteristics may be achieved by gross overdamping of both the seismometer and galvanometer. He has also investigated the application of feedback to a seismograph as an alternate means of obtaining a wide passband [14].

1.3 Seismometer equivalent circuits

It is well known that many mechanical systems may be more conveniently studied by considering their electrical analogs: electrical circuits which satisfy the same differential equation as the mechanical system.

An electromagnetic seismometer is an electromechanical system and may be studied as such. It is, however, much simpler to replace the mechanical part of the system by its electrical analog, leaving a completely equivalent electri-

cal system which may be treated with simple circuit theory.

Such a procedure has long been followed by seismologists, using an equivalent circuit in which a voltage generator represents the ground velocity (Fig.1-5). A simple derivation of this circuit may be found in reference 3.

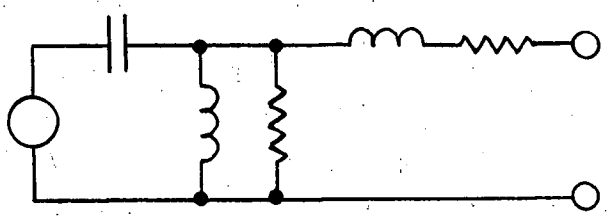

Fig.1-5 Voltage-driven seismometer equivalent circuit.

Kollar and Russell [7] have recently contended that the symmetry inherent in the mechanical resonant system is preserved if the voltage generator present in this rather conventional equivalent circuit is replaced by a current generator. The current driven equivalent circuit is shown in Fig.1-6 and is used throughout this thesis[7].

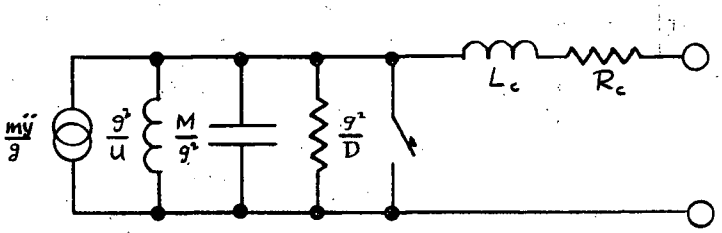

Fig.1-6 Current-driven seismometer equivalent circuit.

The values of the various components are shown and

---

7. This equivalent circuit was originally given by S.A. Scherbatskoy and J. Neufeld, Equivalent electrical networks of seismographs, Geophysics II, 213-242, 1937.

are related to the seismometer constants, spring constant U, damping constant D, mass M, transducer constant g, and to the ground acceleration $\ddot{y}$. R_c and L_c are the resistance and inductance of the coil, and the switch is analagous to a clamp used to prevent the mass from swinging. As Kollar and Russell observe, the electromechanical seismometer and the equivalent circuit are indistinguishable by electrical measurements made at the output terminals.

1.4 Seismometer and seismograph calibration

The calibration of a seismometer involves the determination of its response to sinusoidal ground motions of any period. Willmore [13] has devised a completely electrical method of calibrating electromagnetic seismometers which determines the constants U, D, g, (M is assumed known), and directly produces calibration curves. While Willmore has treated the seismometer as an electromechanical system, Kollar and Russell, using the current equivalent circuit, have enlarged on the Willmore method from a completely electrical point of view. They have also confirmed the validity of the approximations used in the analysis.

For the calibration, the clamped seismometer is placed in the "unknown" position of a Maxwell impedance bridge (Fig.1-7), and the bridge is balanced in the usual manner for "MAIN" input. The balance condition is independent of the frequency and gives the values of R_c and L_c.

Kollar and Russell have shown that with the seismometer unclamped, the ratio of detector outputs for "MAIN"

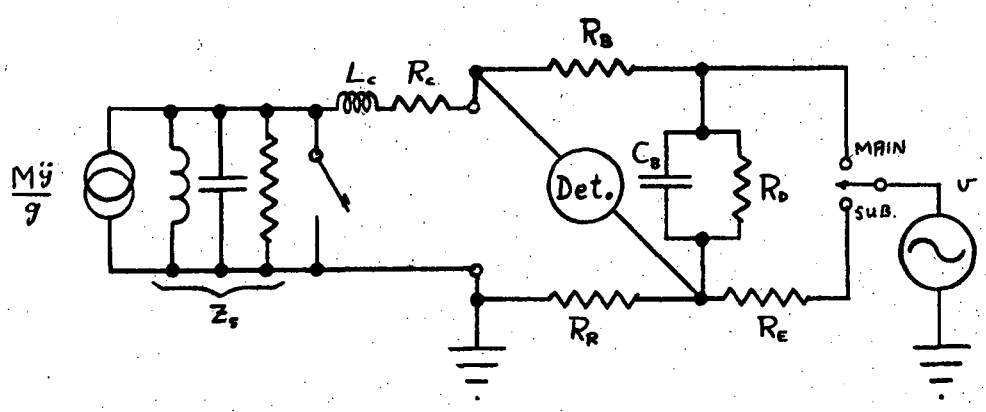

Fig.1-7 Electromagnetic seismometer calibration circuit.

and "SUBSTITUTION" inputs is $\frac{R_E Z_s}{R_R R_B}$ from which $Z_s(\omega)$ may be determined. The positions of the resonant peak and asymptotes of a logarithmic plot of $Z_s(\omega)$ against ω, together with the known suspended mass, determine the values of U, D, and g.

They also show that a potential v applied to the "MAIN" input of the bridge produces the same result as a current generator $\frac{v}{R_B}$ in parallel with Z_s which, comparing with the equivalent circuit, is equivalent to a ground acceleration $\frac{gv}{MR_B}$. With this knowledge, the acceleration sensitivity of the seismometer with the bridge as an attenuator can be plotted, from which the acceleration sensitivity of the seismometer alone can be deduced. The magnification and velocity sensitivity are related to the acceleration sensitivity and may also be determined. If the galvanometer to be used with the seismometer is the bridge detector, the sensitivity curves for the seismograph with the bridge as an attenuating network can be determined.

Willmore has placed a differentiating circuit before

the bridge, enabling the velocity sensitivity to be obtained directly.

Chapter 2 THE APPLICATION OF FEEDBACK TO SEISMOMETERS

2.1 Introduction

It was mentioned in Chapter 1 that Willmore had investigated the application of feedback to a seismograph as a means of obtaining broad band response characteristics.

Feedback has also been used by others to alter the response characteristics of a seismometer, principally to reduce the drift associated with long period instruments. These investigators applied the feedback to the seismometer as opposed to Willmore, whose feedback loop enclosed both the seismometer and galvanometer. In all cases however, an electromagnetic transducer was used to apply the feedback signal to the suspended mass of the seismometer.

In this thesis, feedback will be used solely to alter the overall response of a seismometer, though the method of application will be quite different.

A brief description of the work done by several researchers follows.

2.2 Review of previous work

De Bremaecher et al. [5] have used feedback to eliminate drift in the long period Press and Ewing seismometer in the Rice University direct digitizing seismograph. The input signal to the feedback circuit was a voltage proportional to the ground displacement, derived from the heterodyned frequency of two oscillators tuned by a differential capacitor transducer. The feedback circuit consisted of a

low pass filter (integrator) constructed with an operational amplifier, and was connected to the electromagnetic transducer coil such that the force exerted by the transducer opposed the motion of the mass. The low pass filter ensured that only very long periods were affected, the result being to effectively stiffen the spring for long period signals.

Sutton and Latham [11] have used essentially the same method as de Bremaecker to reduce drift in a long period seismograph designed for unattended operation. The output signal from a differential capacitor transducer, proportional to the mass displacement, was amplified and fed through a low pass filter to the coil of a coil and magnet damping assembly. A centering motor engaged by a trigger circuit was also provided to adjust the suspension if the drift exceeded the capabilities of the feedback current.

In both of the above cases and in general where feedback has been used to reduce the long term drift of a seismometer, the feedback signal can be monitored producing a record of tidal tilts and gravity changes (tidal effects in the vertical component), provided the drift resulting from other sources is negligible.

Tucker [12], on the other hand, has used feedback to shorten the period of a seismometer, which was originally chosen long to improve the signal to noise ratio of the transducer and electrical system, and which lay in the region of interest. He describes a horizontal seismograph designed for the study of microseisms, having nearly flat response to

acceleration for periods ranging from 1.5 sec. to 12.0 sec.. A variable coupling transducer produced a 1kc. signal which was fed through an amplifier and phase sensitive rectifier producing a DC voltage proportional to the mass displacement. This voltage was fed back through a resistor to a transducer coil, producing a restoring force on the mass proportional to its displacement. This effectively increased the spring stiffness, shortening the seismometer period. The feedback resistor was shunted by a capacitor which provided damping, since by the principle of superposition, it produced a current in the coil resulting in a force on the mass proportional to its velocity. The negative feedback also improved the linearity of the amplifier and seismometer, and stabilized sensitivity.

In Willmore's feedback seismograph [14] , the feedback signal was derived from a photoelectric amplifier which produced an output proportional to the galvanometer spot deflection. This output was fed through a resistance-capacitance differentiating network into a secondary transducer coil, producing a force on the mass proportional to the galvanometer spot velocity. Such feedback resulted in a change in the galvanometer reaction unobtainable by other methods, which, with large amounts of damping produced wide band response characteristics.

Chapter 3 THE MAXWELL BRIDGE FEEDBACK SEISMOMETER

3.1 The Maxwell bridge as a means of applying feedback

In applying feedback to a system, it is a simple fact that the feedback signal must be added to the input. This was accomplished by means of electromagnetic transducers in the feedback seismometers just discussed: a current i flowing in the transducer coil causes a mass motion equivalent to that which would be produced by a ground acceleration $\frac{gi}{M}$.

Another method of electrically simulating a ground movement was discussed in § 1.4: a voltage v impressed across the "MAIN" input terminals of the Maxwell bridge used in calibration produces the same effect on the seismometer as a ground acceleration $\frac{gv}{MR_B}$.

Russell (private communication) has suggested it would be possible to add feedback to a seismometer simply by applying the feedback signal to the "MAIN" input terminals of a Maxwell bridge utilized as a permanent attenuating network between the seismometer and the recording system. This method eliminates, in the case of electromagnetic seismometers, the need for a second transducer. Also, when calibrated by Willmore's Maxwell bridge method, corrections usually required when the bridge is removed or replaced by another attenuator are not necessary.

3.2 The effect of feedback on the seismometer

3.2.1 Feedback seismometer transfer function[1].

A circuit diagram showing the application of feedback to a seismometer using the Maxwell bridge is illustrated using transform notation in Fig.3-1. The input ground accel-

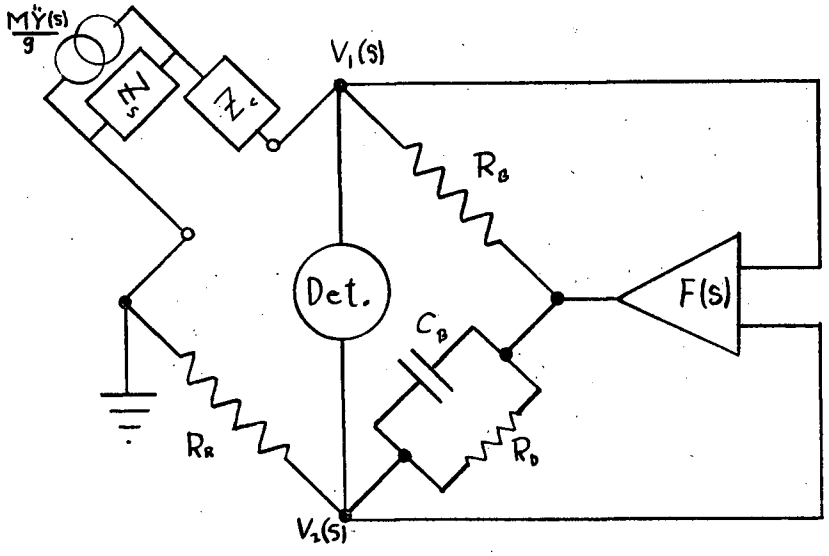

Fig.3-1 Feedback seismometer circuit.

eration is represented by the current generator $\frac{M\ddot{Y}(s)}{g}$ in parallel with $Z_s(s)$.

The output signal $V(s) = V_1(s) - V_2(s)$ is fed through a differential amplifier with transfer function $F(s)$ to the "MAIN" input terminals of the bridge. Since this is equivalent to placing a current generator $\frac{F(s)V(s)}{R_B}$ in parallel with Z_s, the circuit of Fig.3-1 may be replaced with the simplified version shown in Fig.3-2. R_B and Z_B (R_D and C_B in parallel) are required to be large for successful operation of the

---

1. See Appendix C - Feedback.

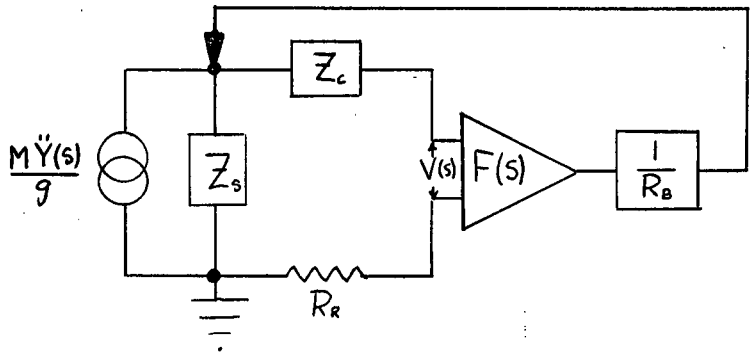

Fig.3-2 Simplified seismometer circuit.

bridge in this manner and have been neglected.

The function of the bridge to change a voltage source $V(s)$ into a current source $\frac{V(s)}{R_B}$ is emphasized by showing the block $\frac{1}{R_B}$ independant of $F(s)$.

Assuming the input impedance of the amplifier to be infinite, there will be no currents flowing through Z_c or R_R , and the transfer function of the seismometer in the bridge without feedback is

$$\frac{V(s)}{I(s)} = Z_s(s) = \frac{g^2 s}{Ms^2 + Ds + U}$$

which is proportional to the acceleration sensitivity of the seismometer since $I(s) = \frac{M\ddot{Y}(s)}{g}$.

The transfer function of the feedback loop is $\pm \frac{F(s)}{R_B}$ and the closed loop transfer function is then

$$Z_s'(s) = \frac{V(s)}{I(s)} = \frac{Z_s(s)}{1 \mp \frac{Z_s(s)F(s)}{R_B}}$$

Rearranging,

$$Z_s'(s) = \left(\frac{1}{Z_s(s)} \mp \frac{F(s)}{R_B}\right)^{-1}$$

Since $Z_s(s)$ is an impedance function, the transfer

function of the feedback seismometer indicates the addition of feedback has effectively added an impedance $\mp \frac{R_B}{F(s)}$ in parallel with Z_s. If $F(s) \propto s^{-1}$, s^0, s, the added impedance is an inductance, resistance, and capacitance respectively, the magnitude of which depends on the gain in the feedback loop and the sign of which depends on the sign of the feedback. Since the resistor, capacitor, and inductor comprising Z_s are respectively related to the damping factor, mass, and spring constant of the seismometer, the effect of adding additional impedances in parallel with Z_s is to alter the values of these parameters, which in turn affects the resonant frequency and damping ratio.

Setting $F(s) = \pm R_B(as^{-1} + b + cs)$, the transfer function of the feedback seismometer is

$$\frac{V(s)}{I(s)} = Z_s'(s) = \frac{g^2 s}{(M \mp g^2 a)s^2 + (D \mp g^2 b)s + (U \mp g^2 c)}$$

$$= \frac{g^2 s}{M's^2 + D's + U'}$$

and

$$\frac{V(s)}{\ddot{Y}(s)} = \frac{Mgs}{M's^2 + D's + U'}$$

where M', D', U', are the effective mass, damping and spring constants. The damping ratio ζ_s' and resonant frequency ω_s' are then $\frac{D'}{2M'\omega_s'}$ and $\sqrt{\frac{U'}{M'}}$ and can be varied at will by adjusting the nature and amount of the feedback.

Due to the instability of gain and distortion generally associated with positive feedback, it will not be discussed. $F(s)$ will henceforth be assigned positive values and negative feedback will be assumed. This does not, however, restrict the capabilities of the system, as both the damping

ratio and resonant frequency can be either increased or decreased by negative feedback.

While an objective of this thesis is to demonstrate the feasability of using a Maxwell bridge to apply feedback to an electromagnetic seismometer, the effects produced by feedback are associated with any feedback seismometer.

3.2.2 Acceleration sensitivity curves.

The acceleration sensitivity of the feedback seismometer to sinusoidal ground motions of angular frequency ω is

$$\left|\frac{V(j\omega)}{\ddot{Y}(j\omega)}\right| = \left|\frac{j\omega M g}{-M'\omega^2 + j\omega D' + U'}\right|$$

At low frequencies, $\left|\frac{V(j\omega)}{\ddot{Y}(j\omega)}\right| \longrightarrow \frac{\omega M g}{U'}$,

at high frequencies, $\left|\frac{V(j\omega)}{\ddot{Y}(j\omega)}\right| \longrightarrow \frac{Mg}{M'\omega}$,

and at the resonant frequency, $\omega = \sqrt{\frac{U'}{M'}}$, and $\frac{V(j\omega)}{\ddot{Y}(j\omega)} = \frac{Mg}{D'}$.

Since M and g are fixed, the height of the resonant peak is altered only by an effective increase in the damping constant. The relative positions of the asymptotes on a logarithmic plot for different values of M', D', U', can be determined from these expressions, allowing a series of acceleration sensitivity curves to be sketched as in Fig. 3-3.

A similar set of sensitivity curves resulting from actual changes in the mass, spring and damping constants is given in Fig.3-4. The corresponding asymptotic and peak expressions for $\left|\frac{E(j\omega)}{\ddot{Y}(j\omega)}\right|$ are derivable from those given above for the feedback seismometer by dropping the primes.

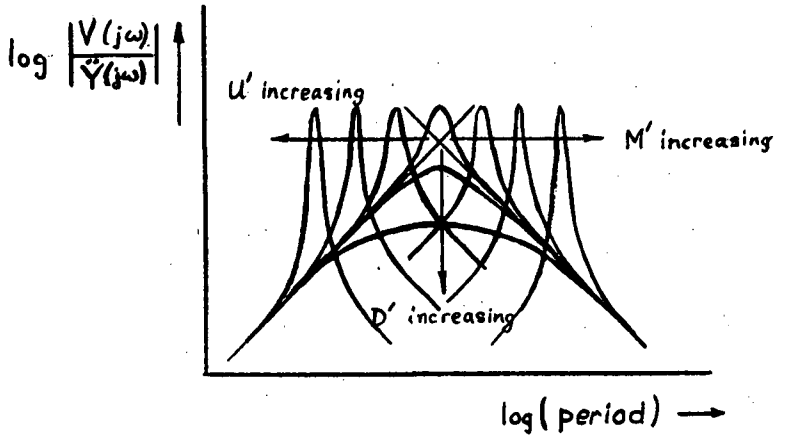

Fig.3-3 Feedback seismometer acceleration sensitivity.

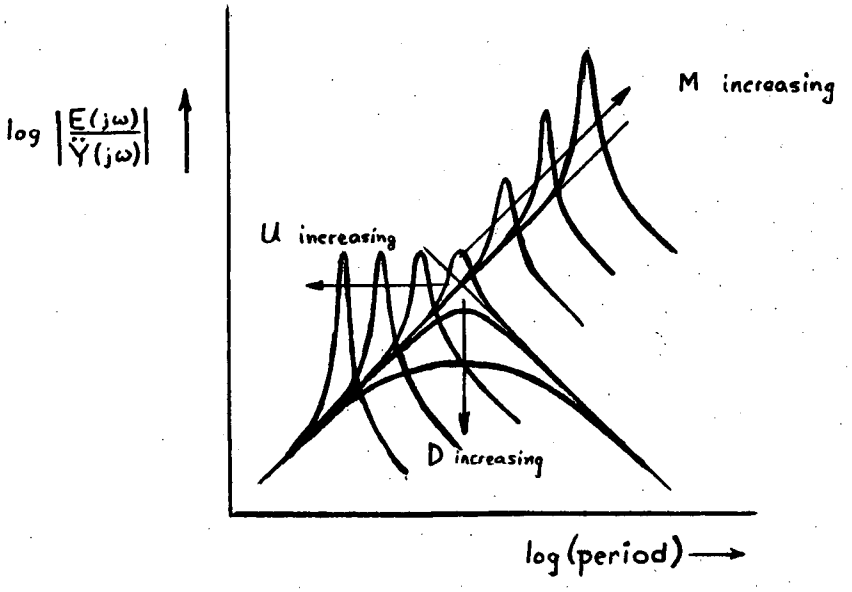

Fig.3-4 Seismometer acceleration sensitivity.

It is apparent from a comparison of Figs.3-3 and 3-4 that while actual and effective increases in both the spring and damping constants have the same effect on the acceleration sensitivity of the seismometer, actual and effective increases in the suspended mass do not. An explanation

of this result is facilitated with the aid of the seismometer equivalent circuit in Fig.3-5. An actual increase in the

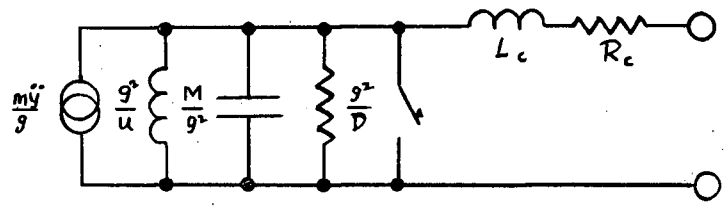

Fig.3-5 Current-driven seismometer equivalent circuit.

spring constant appears in the equivalent circuit as a decrease in the inductance $\frac{g^2}{u}$. An effective increase in the spring constant by the application of feedback was shown in the preceeding section to effectively add an inductance in parallel with Z_s , thereby reducing the total inductance in Z_s . These two means of increasing the spring constant are thus equivalent and an increase by the same factor with either procedure will produce identical acceleration sensitivity curves[2] as indicated in Figs.3-3 and 3-4.

The equivalence of actual and effective increases in the damping constant can similarily be shown.

Now, both actual and effective increases in mass increase the capacitance in Z_s , but an actual mass increase also increases the input current source $\frac{M\ddot{y}}{g}$, resulting in a greater sensitivity to a given ground acceleration as seen in Fig.3-4. The acceleration response of a seismometer with

---

2. In the mechanical system, this is true provided the shift in the equilibrium position of the mass for actual increases does not introduce non-linearities into the operation of the transducer.

a suspended mass M effectively increased by feedback to M' is lower by a factor $\frac{M}{M'}$ than that of a seismometer with an actual mass of M' : the energy extracted from the ground by the instrument depends on the true and not the effective suspended mass.

Since the feedback signal is derived from the seismometer open circuit voltage which is proportional to the velocity of the suspended mass relative to the case, the effective increases in the mass, spring and damping constants are observed only when the mass is in motion. Consequently, the rest position of the suspended mass does not change with effective increases in the mass and spring constant as it would were the changes real. That the damping constant is effectively increased only when the mass is in motion is of no consequence since the damping force is zero when the mass is at rest.

Other operational differences between actual and effective changes in the spring and damping constants arise in noise considerations discussed in §3.2.2(i) and §3.3.3.

3.2.3 Calibration of the feedback seismometer.

The feedback seismometer can be calibrated directly since the bridge used to apply the feedback is capable of converting any number of voltage sources into current sources providing their driving circuits do not interact. A voltage v , so applied to the "MAIN" input of the bridge is equivalent to a ground acceleration $\frac{gv}{MR_s}$. If g is known, the acceleration sensitivity of the feedback seismometer (or

seismograph, if the seismograph recording system is the bridge detector) can be determined. The transducer constant may be determined by disconnecting the feedback circuit and calibrating the seismometer in the bridge as explained in § 1.4.

In practice, to ensure their respective circuits do not interact, the feedback and calibration signals may be added by a summing amplifier[3] before being applied to the bridge.

3.2.4 Root locus diagrams for the feedback seismometer.

The root locus method[4] is often employed in investigating the stability of feedback systems[5]. Its sole purpose here, however, will be to provide graphical analysis of the effect of feedback on the natural frequency and damping ratio of the seismometer since the concept of stability usually associated with feedback control systems and feedback amplifiers has little meaning here. It was shown in §3.2.1 that the application of certain types of feedback to a seismometer resulted only in effectively altering the suspended mass, damping and spring constants. Large loop gains lead only to large deviations in the effective values of these mechanical constants from the original values and not to instabilities as might be expected with a servosystem. The

---

3. See Appendix E - Transfer functions of operational amplifiers.
4. See Appendix D - Root locus method.
5. See Appendix C.2 - Stability of feedback systems.

root locus diagrams, despite their basis of feedback stability criteria, simply provide information on the natural frequency and damping ratio of a seismometer as the various constants, M, D, U, are altered by feedback or by other means.

Root loci are given for the three basic types of feedback discussed, and for linear combinations of these. The feedback transfer function, the mechanical constant altered, and the open loop transfer function from which the root locus plots are constructed are included with each diagram. The seismometer is considered to be initially underdamped ($\zeta<1$), with the result that its poles (which are also the poles of the open loop transfer function) lie at complex conjugate positions in the s-plane.

i) $F(s)=as$, effective mass increase, open loop transfer function $= \dfrac{ag^2s^2}{Ms^2+Ds+U} = \dfrac{Bs^2}{s^2+2\zeta_s\omega_s s+\omega_s^2}$.

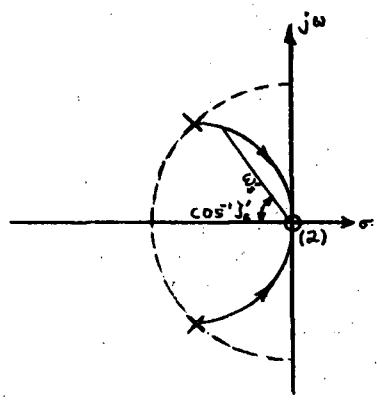

Fig.3-6 Root locus for effective mass increase.

The root locus is the solid arc tangent to the $j\omega$-axis at the origin. As the gain (B) increases from zero at the poles to ∞ at the zeros (the effective mass increases from M to ∞), the damping ratio ζ'_s and the angular natural frequency ω'_s of the feedback seismometer decrease from ζ_s and ω_s to zero.

The poles of seismometers with the same original

resonant frequency but different damping ratios than the seismometer represented above will lie at complex conjugate positions along the dashed arc.

ii) $F(s) = a$, effective damping constant increase, open loop transfer function = $\dfrac{Bs}{s^2 + 2\zeta_s \omega_s s + \omega_s^2}$

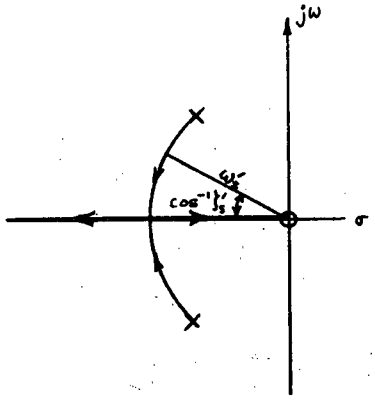

Fig.3-7 Root locus for effective damping constant increase

The root locus lies on the negative real axis, branching out into the s-plane in an arc of radius ω_s centred on the zero at the origin. As the gain increases from 0 , $\omega_s' = \text{constant} = \omega_s$, while ζ_s' increases to 1 at the break-away point, where the seismometer is critically damped, and to values greater than 1 on the axis where the seismometer becomes overdamped. The poles of the overdamped seismometer lie at $-\zeta_s' \omega_s \pm \sqrt{\omega_s \zeta_s'^2 - 1}$.

iii) $F(s) = as^{-1}$, effective spring constant increase, open loop transfer function = $\dfrac{B}{s^2 + 2\zeta_s \omega_s s + \omega_s^2}$

The root locus is a line parallel to the $j\omega$ -axis, indicating ω_s' increase and ζ_s' decrease with increasing gain or spring constant.

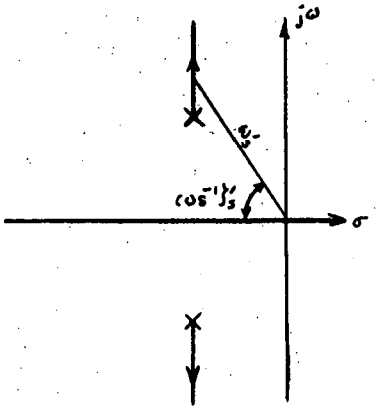

Fig.3-8 Root locus for effective spring constant increase.

iv) $F(s) = (a + bs^{-1}) = bs^{-1}(1+Ts)$, effective spring and damping constant increases, open loop transfer function

$$= \frac{B(1+Ts)}{s^2 + 2\zeta_s \omega_s s + \omega_s^2}$$

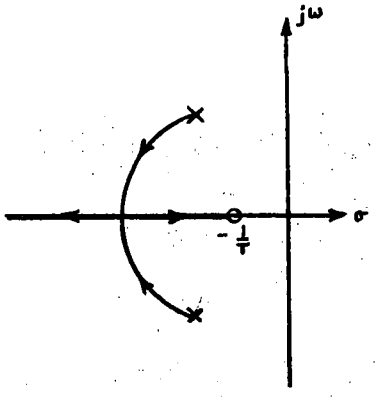

The root locus is an arc centred on the zero at $-\frac{1}{T} = -\frac{b}{a}$.

Fig.3-9 Root locus for effective spring and damping constant increases.

As in the original seismometer, where an increase by the same factor of two of M , D , U , could be interpreted

as a decrease by the same factor of the third, an effective increase in two of M, D, U, by feedback produces similar effects.

An effective increase by the same factor in the spring and damping constants is, from the point of view of seismometer response completely equivalent to an actual mass decrease.

ie., $$\frac{V(s)}{\ddot{Y}(s)} = \frac{Mgs}{Ms^2+Ds+U'} = \frac{Mgs}{Ms^2+aDs+aU} = \frac{(M/a)gs}{(M/a)s^2+Ds+U}$$

However, an effective increase by the same factor of the mass and either of U or D is equivalent to a decrease in the third constant (D or U) accompanied by a decrease by $\frac{M}{M'}$ in the sensitivity which was shown in §3.3.2 to accompany an effective mass increase.

Thus, in Fig.3-9, if $T = \frac{D}{U}$, then $\frac{D'}{D} = \frac{U'}{U}$ and the root locus diagram has the appearance of Fig.3-10. Comparison with the root locus given for effective mass increase (Fig.3-6) confirms the proposition that this case represents an effective mass decrease.

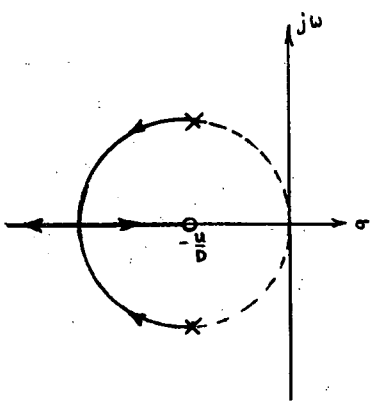

Fig.3-10 Root locus for effective mass decrease.

v) $F(s) = (as + bs^{-1}) = bs^{-1}(1+T^2s^2)$, effective mass and spring constant increases, open loop transfer function

$$\frac{B(1+T^2s^2)}{s^2+2\zeta_s\omega_s s+\omega_s^2}$$

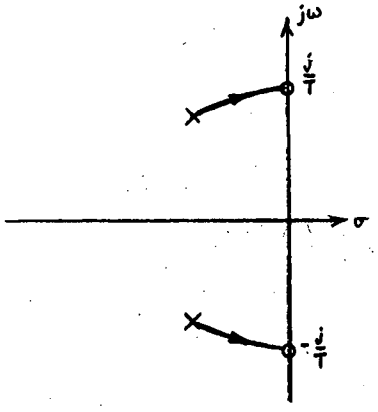

Fig.3-11 Root locus for effective mass and spring constant increases.

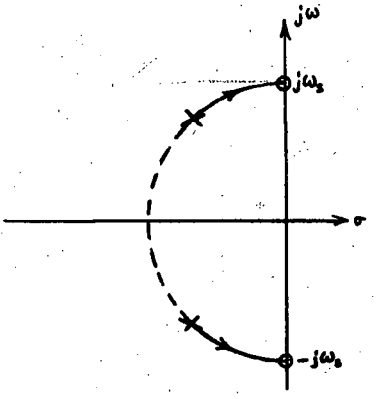

Fig.3-12 Root locus for effective damping constant decrease.

If $T=\frac{1}{\omega_s}$, the root locus takes on the appearance shown in Fig. 3-12, indicating a damping constant decrease (Compare with Fig. 3-4).

vi) $F(s)=(as+b)=b(1+Ts)$, effective mass and damping constant increases, open loop transfer function

$$\frac{Bs(1+Ts)}{s^2+2\zeta_s\omega_s s+\omega_s^2}$$

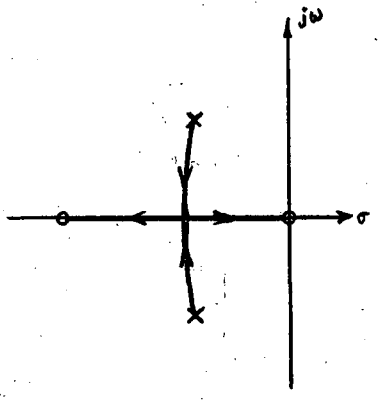

Fig.3-13 Root locus for effective mass and damping constant increases.

If $T = \frac{M}{D}$, the root locus has the appearance shown in Fig.3-14 which comparing with Fig.3-8 indicates a spring constant decrease.

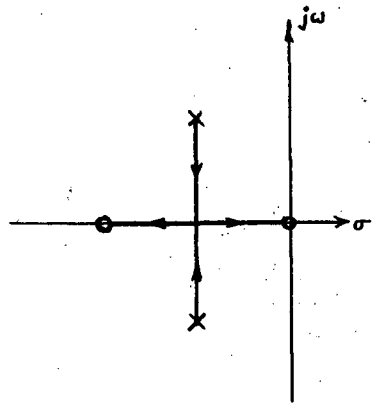

Fig.3-14 Root locus for effective spring constant decrease.

While the root locus diagrams given are essentially qualitative in nature, accurate plots can be constructed for a particular seismometer for quantitative analysis.

It is also instructive to consider the pole positions of the feedback seismometer for the feedback combinations discussed above as resulting from a series of changes, first of one mechanical constant, then of another. For example, if the mass were effectively increased lengthening the period, ζ_s' and ω_s' are determined from the solid arc on the s-plane in Fig.3-15, based on the root locus diagram of Fig.3-6. The gain could be increased until the required natural frequency was ob-

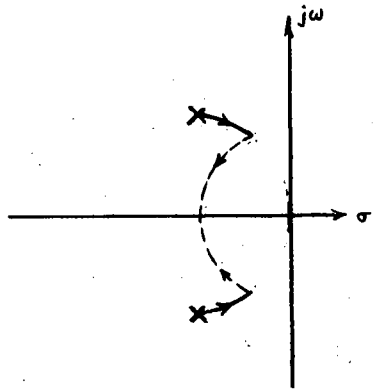

Fig.3-15 Root locus for effective mass increase followed by effective damping constant increase.

tained. If the damping constant were then effectively increased, the poles of the feedback seismometer would move along the dashed line, after the root locus diagram of Fig. 3-7, and the damping ratio could be adjusted to the desired value.

3.3 Instrument noise in the feedback seismometer

3.3.1 Introduction.

Noise in seismometers is generally divided into two broad classes; instrument noise and seismic noise. Seismic noise is any undesirable signal of either artificial or natural origin, which enters the seismometer from the ground. Instrument noise, on the other hand, refers to signals produced in the detector itself and may be attributed to such things as mechanical fatigue and thermo-elastic effects in the suspension elements, and to thermal noise in the associated circuitry and damping system. Barometric changes, air currents and interactions of the seismometer with ambient magnetic fields must also be classed as sources of instrument noise, but will not be discussed since they may be minimized by proper design.

Byrne has extensively dealt with thermal noise in seismic detectors by considering the application to seismometers of two theorems by Nyquist on thermal noise in electromechanical systems. It was shown that the thermal noise present in the seismometer is determined by associating Johnson noise generators with the resistive elements in the equivalent circuit.

While Byrne has used voltage generators with the conventional seismometer equivalent circuit, Kollar and Russell have shown that the analysis is greatly simplified by the use of current generators in the current-driven equivalent circuit.

They have also introduced a means of determining the equivalent input noise of thermal noise sources in complicated networks. This method involves the cancellation of the effect of the noise by an unknown input which is then determined from the requirement that the output be zero by simple circuit theory. They point out that this procedure results in a phase error of π radians but that the phase of a noise source is not significant.

This procedure will be used exclusively in the following paragraphs dealing with thermal noise in the feedback seismometer.

The value of the noise current generator i_n in parallel with $\bar{z}_s$, which produces the same effect at the seismometer output as the noise source in the circuit will be calculated. This input noise current and hence the electrical noise in the seismometer, is then completely equivalent to a ground acceleration $\frac{g i_n}{M}$.

3.3.2 Thermal noise and noise in the feedback loop.

Since the inductive reactance of the transducer coil at frequencies near the seismometer resonant frequency is often negligible compared to the coil resistance, it will be neglected in the following analysis. The capacitor C_B

can then be omitted from the bridge. The external feedback circuitry[6] represented by the differential amplifier with transfer function F can be replaced by a voltage generator FV with internal resistance R_o and the resulting feedback seismometer circuit is shown in Fig.3-16.

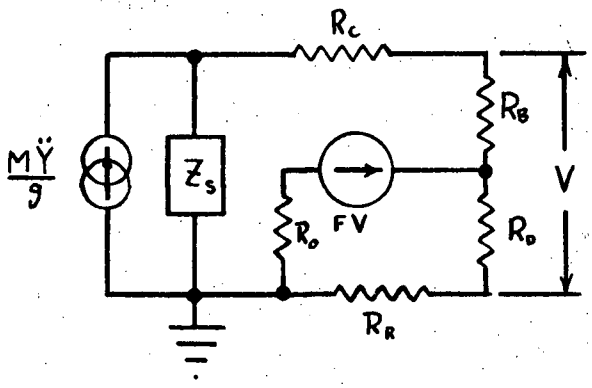

Fig.3-16 Feedback seismometer circuit for noise analysis.

The thermal noise associated with each resistor in the circuit of Fig.3-13 and the noise inherent in the external feedback circuit will be individually considered. R_o will be assumed to be negligible.

i) Thermal noise in "damping resistor" $\frac{g^2}{D}$ in Z_s.

An RMS current generator $\sqrt{\frac{4kT\,df}{g^2/D}}$ where k = Boltzmann's constant, and T is the absolute temperature, placed in parallel with Z_s (and hence with $\frac{g^2}{D}$) represents the thermal noise present in the bandwidth df of the resistance $\frac{g^2}{D}$.

A current generator i_n in parallel with Z_s is considered to be of such a value that it cancels the effect of

---

6. Excluding the bridge.

the noise source. Since it is then required that $V=0$, the voltage generator FV may be replaced by a short circuit, and no current may flow through R_c and R_B (Fig.3-17).

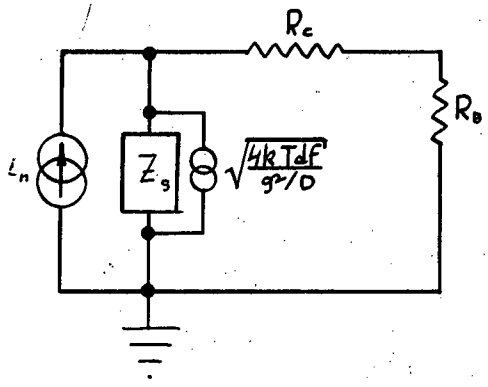

Fig.3-17

Thus $$i_n = -\sqrt{\frac{4kTdf}{g^2/D}}$$

and the thermal noise due to damping remains unchanged by feedback, irregardless of whether the feedback has effectively altered the damping constant.

ii) Thermal noise in R_c .

A voltage generator $\sqrt{4kTR_c df}$ in series with R_c represents the thermal noise in the bandwidth df present in R_c (Fig.3-18).

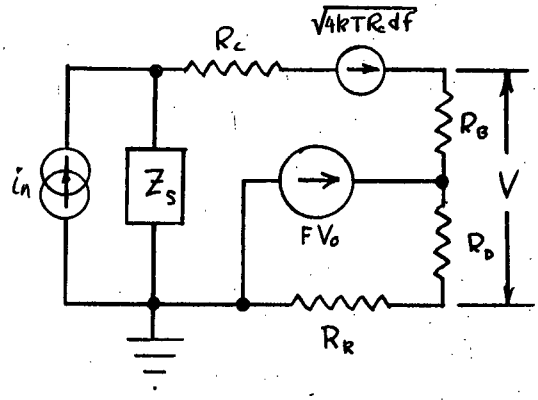

Fig.3-18

If it is balanced by the input noise current i_n ,

then $V=0$ and the generator FV may be replaced by a short circuit. Also, no current can flow through R_B, with the result that

$$i_n = -\frac{\sqrt{4kTR_c\,df}}{Z_s}$$

iii) Thermal noise in R_B.

Representing the thermal noise by a voltage generator $\sqrt{4kTR_B\,df}$ in series with R_B, and requiring V to be zero leads to the circuit shown in Fig.3-19 and the requirement $iR_B = \sqrt{4kR_B\,df}$

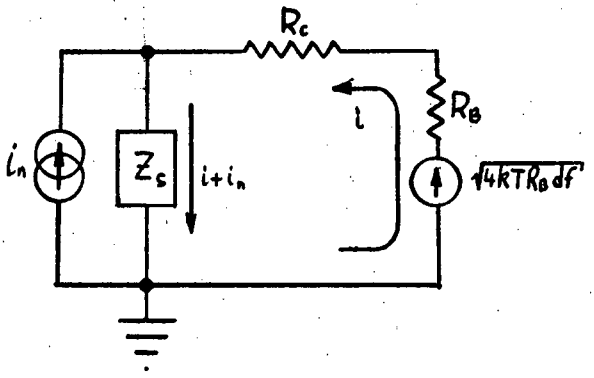

Fig.3-19

Kirchhoff's law gives

$$i(R_B + R_c) + (i + i_n)Z_s = \sqrt{4kTR_B\,df}$$

These two equations can be solved for i_n:

$$i_n = -\frac{\sqrt{4kTR_B\,df}\,(R_c + Z_s)}{R_B Z_s}$$

iv) Thermal noise in R_D.

The thermal noise associated with R_D is represented by the voltage generator $\sqrt{4kTR_D\,df}$ in series with R_D. If $V=0$

then in Fig.3-20

$$i_1 (R_B + R_D) + i_2 R_D - \sqrt{4kTR_D df} = 0$$

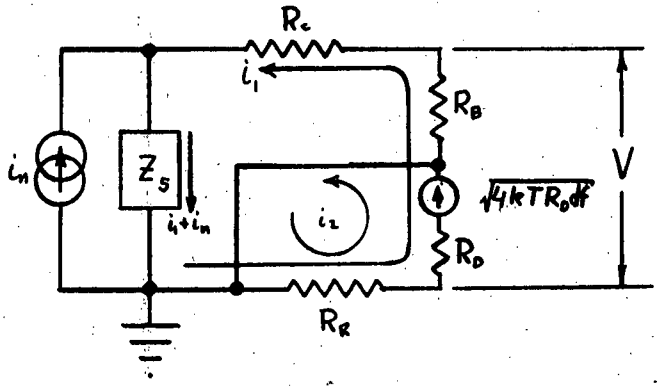

Fig. 3-20

Kirchhoff's law gives two more equations,

$$(i_n + i_1) Z_s + i_1 (R_R + R_D + R_B + R_c) + i_2 (R_R + R_D) = \sqrt{4kTR_D df}$$

$$(i_1 + i_2)(R_R + R_D) = \sqrt{4kTR_D df}$$

These three equations give

$$i_n = -\frac{\sqrt{4kTR_D df}}{Z_s} \cdot \frac{R_R (Z_s + R_B + R_c)}{R_B (R_R + R_D)}$$

v) Thermal noise in R_R.

A voltage generator $\sqrt{4kTR_R df}$ in series with R_R represents the thermal noise associated with R_R. The circuit shown in Fig.3-21 and the requirement

$$i_1 (R_B + R_D) + i_2 R_D = 0$$

result if V is to be zero.

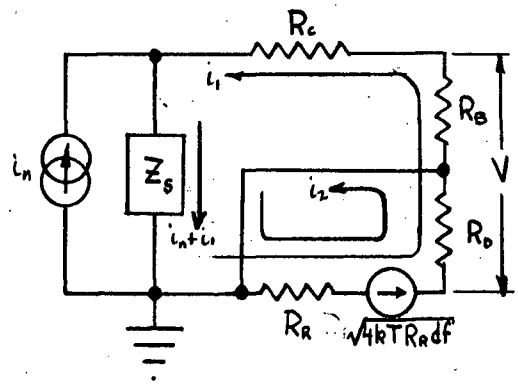

Fig.3-21

Kirchhoff's laws give

$$(i_n+i_1)Z_s + i_1(R_c + R_B + R_D + R_R) + i_2(R_R + R_D) = \sqrt{4kTR_R df}$$

$$(i_1 + i_2)(R_R + R_D) = \sqrt{4kTR_R df}$$

Solving these three equations gives

$$i_n = \frac{\sqrt{4kTR_R df}}{Z_s R_B} \cdot \frac{R_D(R_c + R_B + Z_s)}{(R_R + R_D)}$$

vi) Noise in external feedback circuitry.

Consider an RMS noise voltage ϵ to be present in the input of the voltage generator of Fig.3-16. This is equivalent to a noise ϵ across the input of the differential amplifier representing the feedback circuit. If V is zero, then this noise can be represented by a voltage generator ϵF as shown in Fig.3-22.

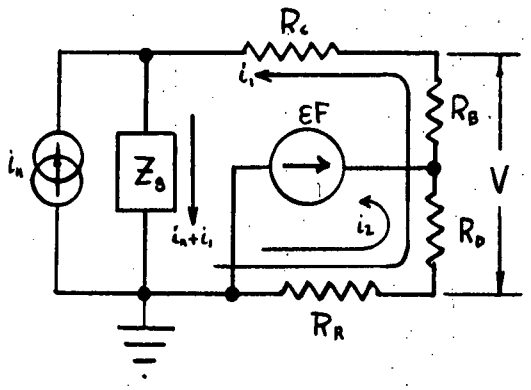

Fig.3-22

Also, if $V = 0$,

$$i_1 (R_D + R_R) + i_2 R_D = 0$$

Kirchhoff's law gives

$$i_1 (R_R + R_D + R_B + R_c + Z_s) + i_2 (R_R + R_D) + i_n Z_s = 0$$

$$(i_1 + i_2)(R_R + R_D) = -\mathcal{E}F$$

These equations may be solved for i_n giving

$$i_n = -\frac{\mathcal{E}F}{Z_s} \cdot \frac{R_D (Z_s + R_c + R_B) - R_B (R_R + R_D)}{R_B (R_R + R_D)}$$

The total equivalent input noise current in the bandwidth df due to the above mentioned sources is found by taking the square root of the sum of the squares of the individual RMS noise currents. The corresponding input ground acceleration in the bandwidth df is then $\frac{g}{M}$ times the total input noise current.

The equivalent ground acceleration in a specified bandwidth due to these sources can be calculated by integrating the corresponding expression for bandwidth df over

the required frequency band.

3.3.3 Drift in the feedback seismometer.

It was shown in §3.5.2 that the equivalent input noise associated with the thermal noise in the seismometer due to damping was unchanged by the application of feedback.

In general, the equivalent input noise of a system remains the same before and after feedback is applied[7].

Thus, drifts due to thermo-elastic effects and mechanical fatigue in the spring which can be represented as long period input ground accelerations, are unchanged by the application of feedback. Increasing the period of the seismometer by feedback will, however, increase its sensitivity to long term drift, but if the drift is originally negligible with respect to long period signals, it will remain so.

---

7. Proof in Appendix C.

Chapter 4 EXPERIMENTAL VERIFICATION OF FEEDBACK THEORY

4.1 The Willmore Mk.I seismometer

Experimental verification of the theory presented in Chapter 4 was carried out using a Willmore Mk.I seismometer, formerly a standard in the Canadian seismograph network[1]. The Willmore Mk.I is a portable, short period seismometer, capable of both vertical and horizontal operation. Its suspended mass of 4.26 kg is a cylindrical permanent magnet, constrained to move axially along the seismometer axis by five spokes, which also provide the restoring force in horizontal operation. Two triangular leaf springs support the mass for vertical operation. Minor period adjustments are readily made to obtain a resonant period of 1 sec. in both the horizontal and vertical positions. The electromagnetic transducer consists of a coil, fastened to the base plate of the seismometer, which enters a circular gap between the suspended magnet's concentric pole pieces. In the instrument used, the coil was wound on a special aluminum former which provided some degree of eddy current damping. Additional damping is usually obtained by shunting the coil with a suitable resistance. An external thumb screw enables the magnet to be clamped against the bottom stop during transportation.

---

1. Now replaced by the Willmore Mk.II.

The seismometer was operated solely in the horizontal position for these experiments.

It was calibrated using a Maxwell bridge by the method explained in §1.4. The resulting calibration curve is shown in Fig.4-1, with the ordinate values adjusted to give the value of Z_s in ohms. The various seismometer constants were

M = suspended mass = 4.26 kg

D = damping constant = 14.2 Nsec/m

U = spring constant = 168 N/m

g = transducer constant = 161.0 volt sec/m

R_c = coil resistance = 1020Ω

L_c = coil inductance[2] = 1.18 h

ζ_s = damping ratio = 0.266

The values of the resistor, capacitor, and inductor representing the mechanical part of the seismometer, Z_s, in the current-driven equivalent circuit (Fig.1-6) were respectively 1825Ω, 165μF, and 154 h.

4.2 Calibration and feedback circuitry

The bridge used to apply feedback to the seismometer was of course, the same bridge used to calibrate it. The resistances and capacitance comprising the bridge were measured on a General Radio impedance bridge and were

---

2. L_c was found to vary with frequency. The value given was determined at the seismometer resonant frequency, 1cps.

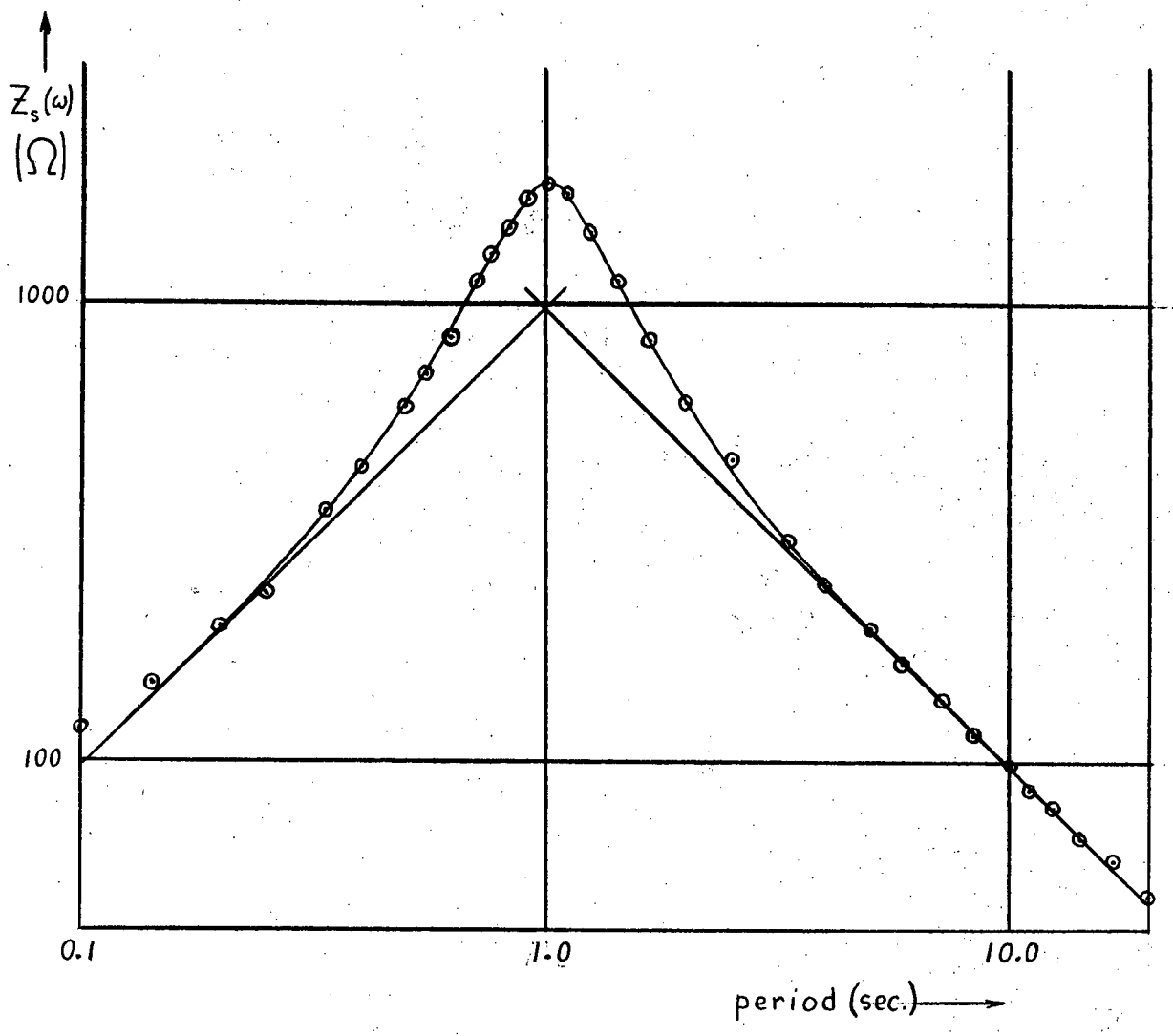

Fig.4-1 Calibration Curve ($Z_s(\omega)$) for Willmore Mk.I Seismometer.

R_B = 102.2k, R_R = 105Ω, R_D = 10.5k, C_B = 0.11μF. The substitution resistor R_E = 10.0k was used in calibration only.

The output from the bridge was fed through a switch to an Astrodata nanovoltmeter operated as a floating preamplifier to a Tektronix #502 oscilloscope. The output of a KROHN-HITE model 440AR ultra-low frequency oscillator which provided the calibrating voltage, was connected through a 40db attenuator to the switch leading to the preamplifier and oscilloscope where it could be measured.

The preamplifier gain was fixed at 100 to avoid bandwidth differences between ranges. Since all data required were ratios of two signals, the corner frequency of the amplifier at ~3.2 cps did not affect the results.

A block diagram illustrating the application of feedback to the seismometer is given in Fig.4-2. It also illustrates the method of determining the acceleration sensitivity of the feedback seismometer explained in § 3.2.3.

Vacuum tube operational amplifiers and coefficient potentiometers of a Heathkit Model C Analog Computer were used to provide the gain and to perform the required mathematical operations in the feedback loop. 10% capacitors and 5% resistors were used with the amplifiers.

It was found that these amplifiers acquired a dc offset when confronted with a capacitive load such as the Maxwell bridge. The closing of the feedback loop further enhanced the problem. This effect could be overcome if the

feedback circuit consisted of an integrator, by placing a 330Ω resistance in series with C_B. The addition of this resistance did not affect the operation of the bridge.

This procedure failed however, when a differentiator comprised the feedback circuit, and it was necessary to remove C_B from the bridge. This did affect the operation of the bridge at higher frequencies (above 3 cps) but as the purpose of the differentiator in the feedback loop was to decrease the natural frequency, the absence of C_B was not important.

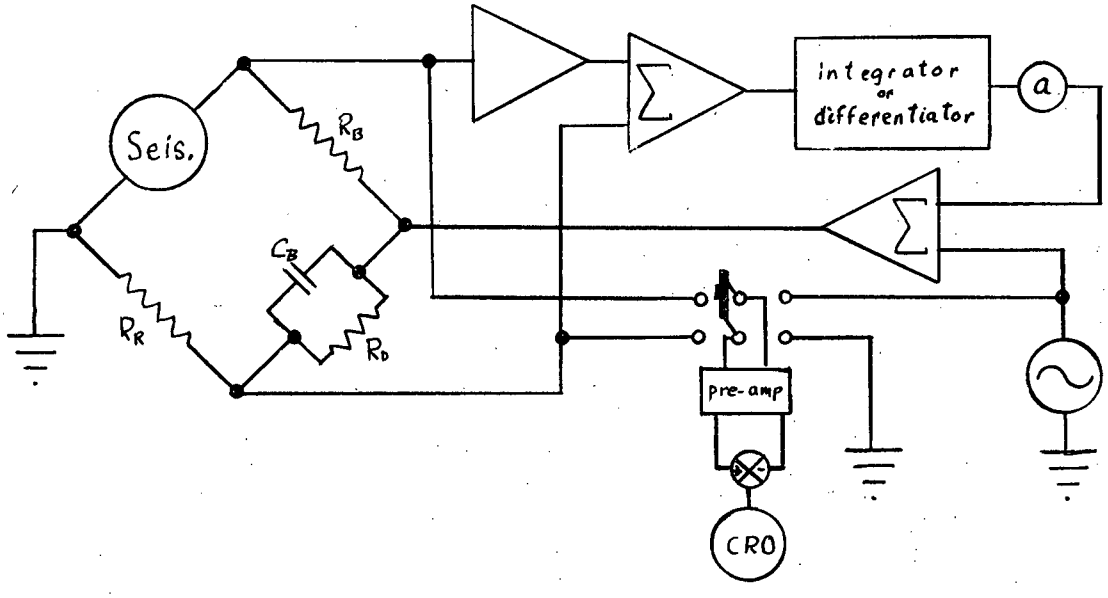

Fig.4-2 Experimental feedback and calibration schematic.

4.3 Experimental results

Several experimentally determined acceleration sensitivity curves for the feedback seismometer with different effective masses, spring and damping constants are compared with the original acceleration sensitivity curve of the seismometer in Figs.4-3a and 4-3b. The curves of Fig.4-3a

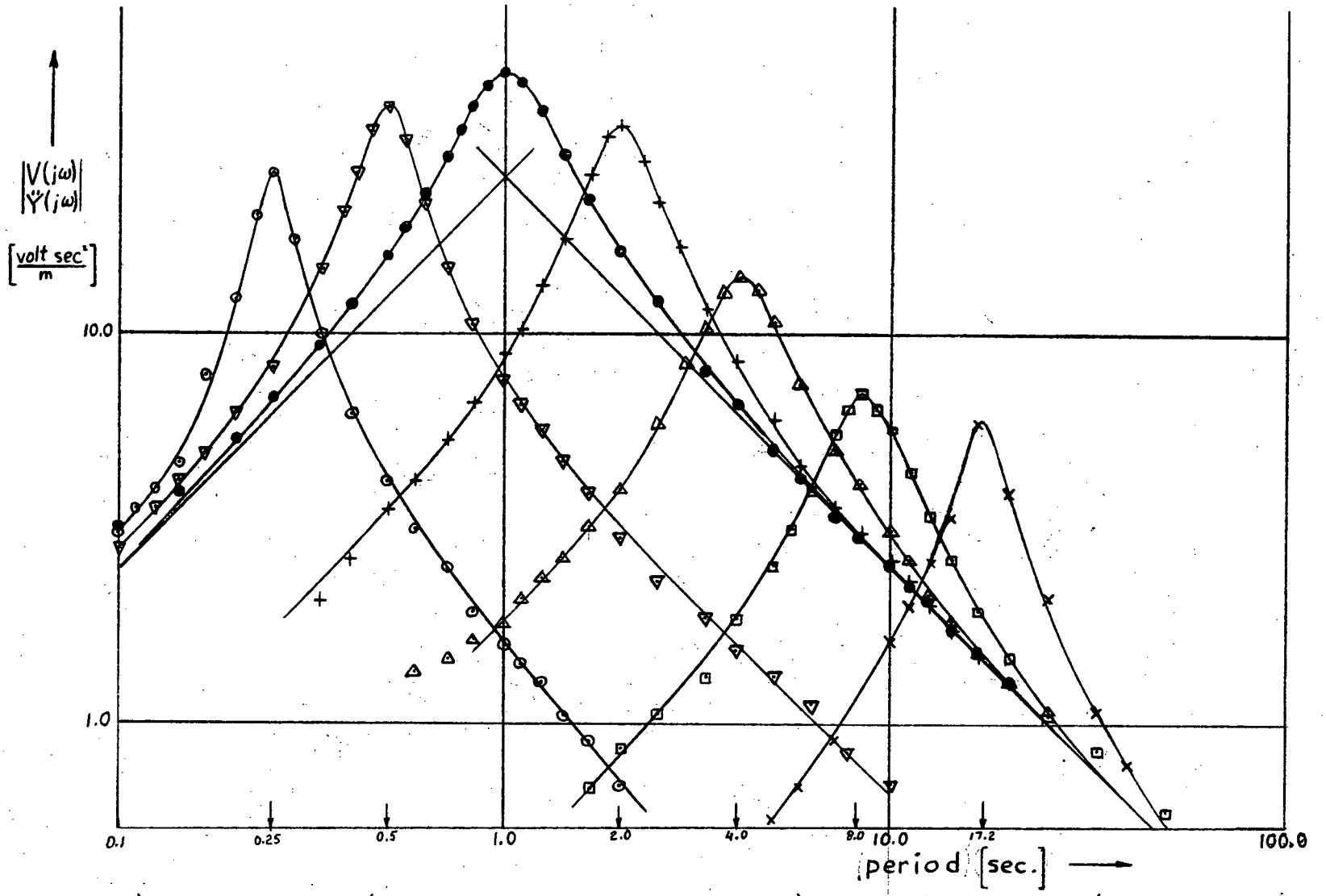

a) acceleration (periods greator than 1 sec.) and displacement (periods less than 1 sec.) feedback

Fig.4-3 Experimental acceleration sensitivities of feedback seismometer.

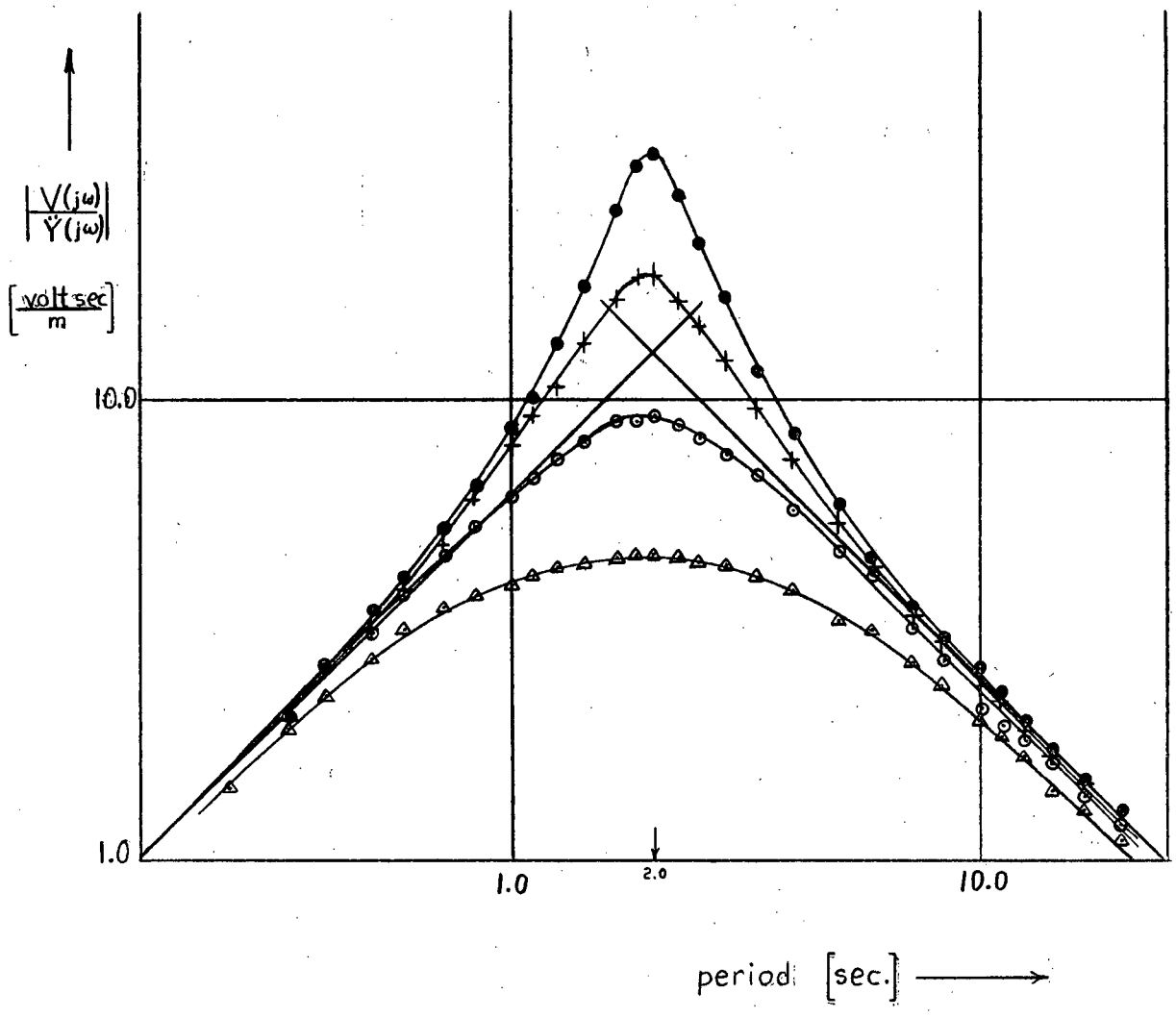

b. Velocity feedback applied to 2 sec. period feedback seismometer.

Fig.4-3 Experimental acceleration sensitivities of feedback seismometer.

with resonant periods greater than 1 sec. were obtained with negative acceleration feedback (effective spring constant increase). The curves of Fig.4-3b display the capabilities of feedback in damping the seismometer and were obtained by adding negative velocity feedback to the 2 sec. resonant period feedback seismometer.

Tables 4-1 and 4-2 contain various information about the feedback seismometers which the curves represent. All information present in the tables was derived from the curves and from the original values of the various constants. T_θ is the resonant period of the feedback seismometer, and is determined from the position of the peak of the acceleration sensitivity curves.

While the curves of Fig.4-3a indicate an increase in the damping constant (see Table 4-1 and Fig.3-3), velocity feedback was not applied to the seismometer and the cause of the additional damping is unknown. One possibility investigated was that of an unwanted phase shift in the feedback loop. A phase lag in the differentiating network and a phase lead in the integrating network could introduce a component of velocity feedback. As will be explained later, the differentiator and integrator used in the feedback loop have high and low frequency cutoffs respectively, resulting in phase differences of the required sign to introduce damping. In Table 4-1, ϕ is the magnitude of the phase angle required to produce the damping observed in the various curves. The values of ϕ were calculated from one of

T_o [sec.]		0.25	0.5	1.0*	2.0	4.0	8.0	17.2
added impedance	R [Ω]	1920	5530	—	4800	758	325	258
	L [h.]	10.1	51.4	—	—	—	—	—
	C [μF]	—	—	—	492	2460	10,400	48,600
effective	M [kg]	4.26*	4.26*	4.26*	17.0	68.2	273	1265
	D $\left[\frac{N\,sec}{m}\right]$	27.7	19.1	14.2*	19.6	48.4	94.0	115.5
	U $\left[\frac{N}{m}\right]$	2690	672	168*	168*	168*	168*	168*
ζ		0.129	0.178	0.285*	0.184	0.226	0.219	0.125
ϕ [°] ‡		0.3	0.55	—	22.84	28.15	16.5	4.6

* Original value.
‡ Defined in text on page 47.

Table 4-1 Information pertaining to acceleration sensitivity curves of Fig. 4-3a.

$$\phi = \tan^{-1}\left(\frac{\Delta D}{\Delta U}\right) \quad \text{or} \quad \phi = \tan^{-1}\left(\frac{\Delta D}{\Delta M}\right)$$

where ΔM, ΔD, ΔU represent the effective increases in each of the parameters M, D, U. ϕ was found to be too large in all cases except for T_o = 0.5 sec. and 0.25 sec., for which it was too small. ϕ in general was also too large to be associated with phase shifts in the operational amplifiers used.

curve no.†		1	2	3	4
added impedance	$R\ [\Omega]$	4800	1215	440	197
	$L\ [h.]$	—	—	—	—
	$C\ [\mu F.]$	492	492	492	492
effective	M kg	17.0	17.0	17.0	17.0
	$D\ \left[\frac{N\cdot sec}{m}\right]$	19.6	35.5	73.0	146
	$U\ \left[\frac{N}{m}\right]$	168*	168*	168*	168*
ζ		0.184	0.336	0.691	1.38

† Curves are numbered consecutively from least damped.
* Original value.

Table 4-2 Information pertaining to acceleration sensitivity curves of Fig.4-3b.

Since ϕ is small for T_o = 0.5 sec. and 0.25 sec. for which C_B was retained in the bridge, and large for the other cases, for which C_B was removed from the bridge, it is possible that the coil inductance of the seismometer combined with the above possibilities to produce the required phase shifts. The differentiating circuit used to obtain the curve for T_o = 2.0 sec. had different characteristics from the others which may explain the deviation from the tendency of ϕ to increase towards the higher resonant frequencies.

4.4 Integrator, differentiator and summing amplifier[3]

The summing amplifiers were constructed with megohm resistances, and the multiplications by 10 (recommended limit with these amplifiers) were accomplished with 100k and 1 megohm resistances.

Although operational amplifiers are theoretically capable of ideal integrations and differentiations, the presence of noise requires the use of practical differentiators and integrators. The integrating circuit used is shown in Fig.4-4a and a logarithmic plot of the gain in Fig.4-4b.

The transfer function of this integrator is

$$\frac{R_2}{R_1} \cdot \frac{1}{1+T_2 s}$$

where $T_2 = R_2 C_2$. While this reduces to an ideal integrator only if $R_2 = \infty$, it approximates an ideal integrator for

---

3. See Appendix E - Transfer functions of operational amplifiers.

angular frequencies ω such that $\omega T_2 \gg 1$.

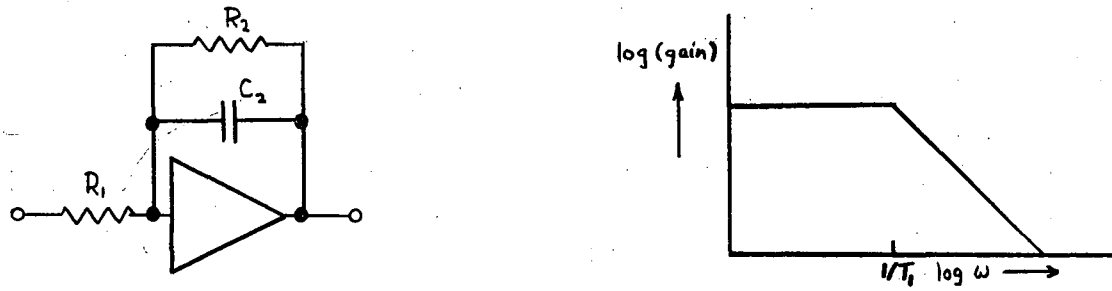

a) circuit b) gain

Fig.4-4 Integrator used in experimental work.

The values of the resistances and capacitance used were R_1 = 100k, R_2 = 1 meg., and C_2 = 2.0μF., with the corner period of 12.4 sec.

The differentiating circuit used is shown in Fig. 4-5a and a logarithmic plot of the gain in Fig.4-5b.

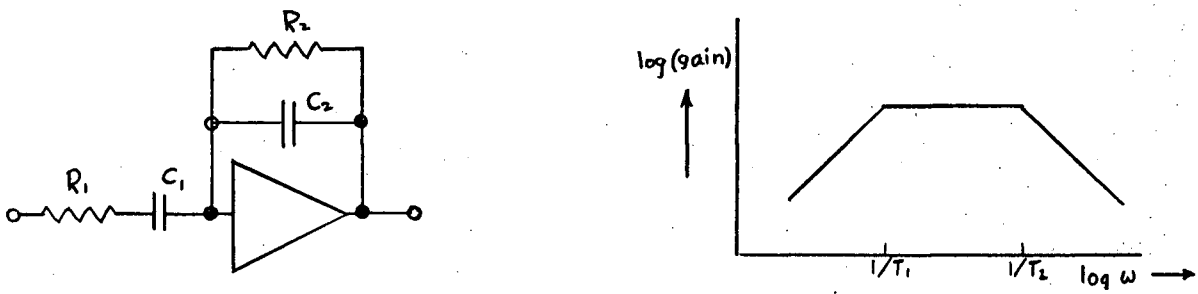

a) circuit b) gain

Fig.4-5 Differentiator used in experimental work.

The transfer function of this differentiator is

$$\frac{R_2 C_1 s}{(1+T_1 s)(1+T_2 s)}$$

where $T_1 = R_1 C_1$, $T_2 = R_2 C_2$, with $T_1 > T_2$. This reduces to an ideal differentiator only if $C_2 = 0$ and $R_1 = 0$, but approximates an ideal differentiator for angular frequencies

such that $\omega T_1 << 1$.

The values of the resistances and capacitances used were: R_1 = 100k, R_2 = 1meg., C_2 = 0.01μF, and C_1 was for T_o = 2.0 sec. 0.143μF, and for the other three curves, 1.0μF. The corner period at $\frac{1}{2\pi T_1}$ was 0.09 sec. (11.1 cps) and 0.63 sec respectively for the two values of C_1, and at $\frac{1}{2\pi T_2}$ was 0.063 sec. (15.9 cps).

It was necessary to keep the corner frequencies of the low frequency cutoff of the integrator and the high frequency cutoff of the differentiator out of the frequency ranges of interest. If this was not done, the order of the system increased and the effective spring constant and mass became functions of frequency, distorting the sensitivity curves.

While it is possible to obtain direct feedback with a separate operational amplifier and add it with a summing amplifier to the other feedback signals to produce damping, combinations of direct feedback, with differentiated feedback are possible with one amplifier by shunting R_1 and C_1 in the differentiator by a resistor as shown in Fig. 4-6a. A logarithmic plot of the gain is given in Fig.4-6b.

The transfer function is

$$\frac{R_2(1+Ts)}{R_1'(1+T_1s)(1+T_2s)}$$

where $T = T_1 + R_1'C_1$. For angular frequencies $\omega < \frac{1}{T}$, the differentiator transfer function is $\frac{R_2(1+Ts)}{R_1'}$ which gives velocity and acceleration feedback (remembering that the seismometer output is proportional to the velocity of the mass).

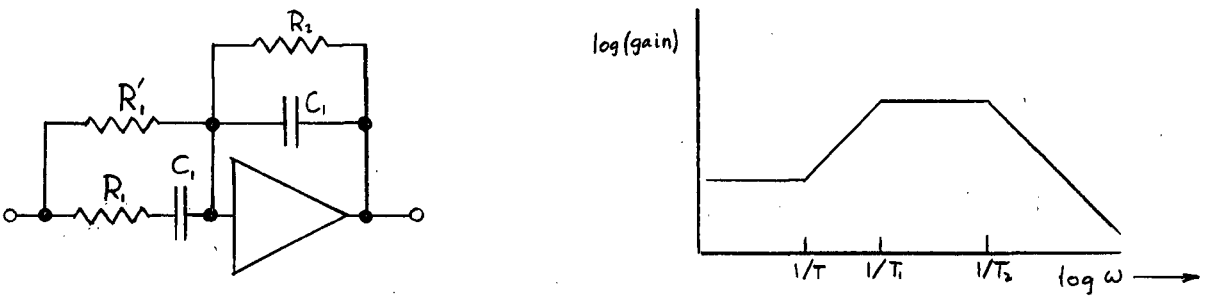

a) circuit b) gain

Fig.4-6 Single amplifier producing combination of direct and differentiated feedback.

The velocity feedback coefficient is $\frac{R_2}{R_1'}$ and varies with R_1', while the acceleration feedback coefficient is $\frac{R_2C_1(R_1+R_1')}{R_1'}$ and also varies with R_1'. However, if as illustrated in Fig. 4-7, R_1 is appropriately chosen, the damping may be varied through a wide range without affecting the acceleration feedback coefficient and hence the resonant period of the feedback seismometer.

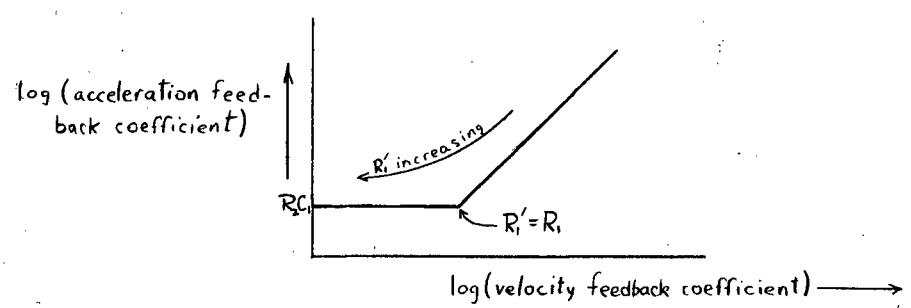

Fig.4-7 Acceleration feedback coefficient versus velocity feedback coefficient for operational amplifier of Fig.4-6a.

4.5 Practical root locus diagrams

Since the differentiator and integrator actually used differ from the ideal cases dealt with in the theory

in Chapter 3, it is reasonable to expect the root locus diagrams to take on a different appearance. However, as pointed out in §4.3, if the time constants were correctly chosen, the practical circuits behave ideally for the frequency ranges of interest. Thus, while the root locus plots contain extra poles, zeros, and branches, the final results are essentially the same as shown in the following figures.

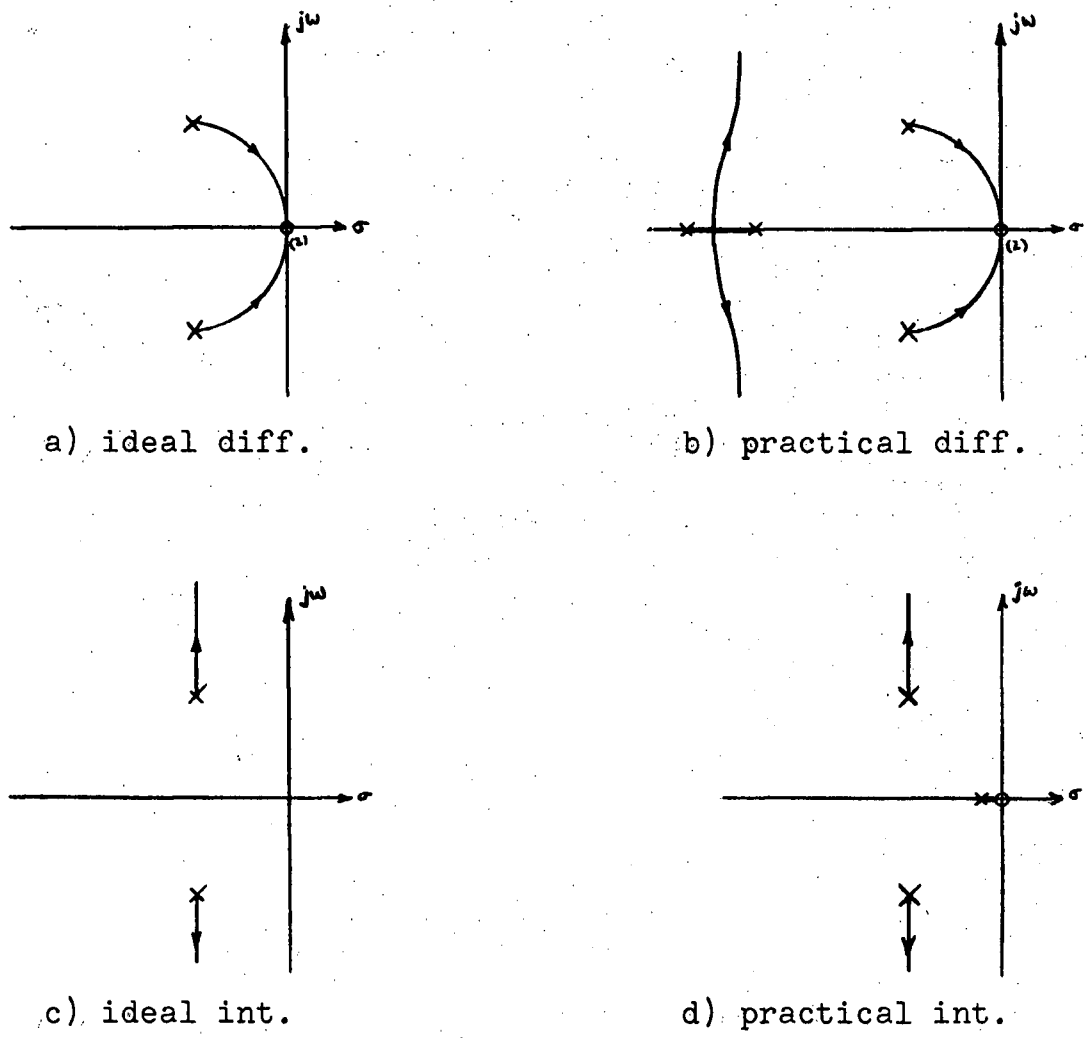

a) ideal diff. b) practical diff.

c) ideal int. d) practical int.

Fig.4-8 Comparison of ideal and practical root loci.

Chapter 5 CONCLUSION

It has been shown that by application of negative feedback, the shape and position of the response curves of a seismometer can be altered at will, with regard to the damping and natural period. Negative acceleration feedback applied to the suspended mass of a seismometer effectively increases the mass, lengthening the period, while negative displacement feedback shortens the period by effectively stiffening the spring. The damping factor is effectively increased by negative velocity feedback. Similar results follow the application of negative feedback to pendulum seismometers in which moments of inertia are considered in place of suspended masses.

The ability to lengthen or shorten the resonant period and hence shift the response band of a seismometer by the application of feedback will allow a particular instrument to be adapted to various research projects. The Willmore Mk. II seismometer with a built in period adjustment, has a period range of from 0.6 sec. to 3.0 sec. but this is far less than the capabilities of a seismometer with feedback.

While the amount of electromagnetic damping which can be applied to a seismometer is restricted by the field strength of the transducer magnet, the use of negative feedback enables any desired degree of damping to be obtained. It appears then, that the feedback method might be an excellent means of grossly overdamping seismometers to achieve the

broad band characteristics desired for magnetic tape recording.

The actual shape of the response curves, aside from differences in damping, can be altered with feedback if the restriction that the unloaded feedback seismometer be a second order system is removed. The application of displacement feedback through a low pass filter to reduce drift in long period seismometers, as described in Chapter 2, results in a third order system. In these seismometers, the spring constant becomes a function of period, increasing with longer periods. The acceleration response of the feedback seismometer at long periods, determined by the spring constant, drops off at a rate greater than the normal 6db/octave.

The use of the Maxwell bridge in applying feedback to an electromagnetic seismometer through the transducer coil terminals obviates the need of a second transducer and its necessary calibration.

The Maxwell bridge also permits direct calibration of the the feedback seismometer and seismograph based on the method of Willmore. The corrections usually required when the bridge used in calibration is replaced by another attenuator are not required, since the bridge is a permanent feature of the feedback seismometer.

The final step in the theory presented here is being taken by O. G. Jensen of the Dept. of Geophysics at U.B.C. in the building of a seismograph incorporating the feedback methods presented.

BIBLIOGRAPHY

1. Benioff, H., Earthquake seismographs and associated instruments, Advances in Geophysics 2, 219-275, 1955.

2. Bohn, E.V., The Transform Analysis of Linear Systems, Addison-Wesley Publishing Co. Inc., Reading, Mass., 1963.

3. Brunelli, B.E., and V.V. Alekseev, Seismograph system with feedback, Bull.(Izv.) Acad. Sci. USSR, Geophys. Ser., No 1, 524-527, 1959.

4. Byrne, C.J., Instrument noise in seismometers, Bull. Seismol. Soc. Am. 51, 69-84, 1961.

5. De Bremaecker, J.Cl., P. Donoho, and J.G. Michel, A direct digitizing seismograph, Bull. Seismol. Soc. Am. 52, 661-672, 1962.

6. Hodgson, J.H., Earthquakes and Earth Structure, 60-69, Prentice Hall Inc., Englewood Cliffs, New Jersey, 1964.

7. Kollar, F., and R.D. Russell, Seismometer analysis using an electric current analog, (Submitted for publication in Bull. Seismol. Soc. Am.).

8. Richter, C.F., Elementary Seismology, 210-231, W.H. Freeman and Co. Inc., San Fransisco, 1958.

9. Rykov, A.V., The effect of feedback on the parameters of a pendulum, Bull.(Izv.) Acad. Sci. USSR, Geophys. Ser., No.2, 636-640, 1963.

10. Savant, C.J., Basic Feedback Control System Design, 81-123, McGraw-Hill Book Company Inc., New York, 1958.

11. Sutton, G.H., and G.V. Latham, Analysis of a feedback-controlled seismometer, J. Geophys. Res. 69, 3865-3882, 1964.

12. Tucker, M.J., An electronic feedback seismometer, J. Sci. Instr. 35, 167-179, 1958.

13. Willmore, P.L., The application of the Maxwell impedance bridge to the calibration of electromagnetic seismographs, Bull. Seismol. Soc. Am. 49, 99-114, 1959.

14. Willmore, P.L., Some properties of heavily damped electromagnetic seismographs, Roy. Ast. Soc. Geophys. J. 4, 389-404, 1961.

15. Willmore, P.L., The detection of earth movements, Runcorn, S.K., (ed.), Methods and Techniques in Geophysics, 230-276, Interscience Pub. Ltd., London, 1959.

Appendix A ELECTROMAGNETIC TRANSDUCER

A.1 Theory

The electromagnetic transducer converts mechanical energy into electrical energy by application of Faraday's law of electromagnetic induction. A coil, often attached to the suspended mass, lies in the field of a permanent magnet attached to the seismometer frame[1]. If the mass and coil move with a velocity v relative to the frame, an emf gv is induced across the open terminals of the coil where g is the transducer constant and is related to the magnetic flux threading the coil and to the number of turns in the coil.

If the coil is not open circuited, but is connected to a resistive attenuating network or is shunted by a resistor to produce electromagnetic damping (A.2) the output voltage is no longer gv but is modified by the coil and shunt impedances. In these cases, if the inductive reactance of the coil is not negligible at the frequencies of signals being induced by the ground motion, the seismometer becomes a third order system, changing the response characteristics derived in Chapter 1.

The electromagnetic transducer also converts electrical energy into mechanical energy: a current i flowing in the coil causes a force gi to be exerted on the suspended

---

1. An arrangement exactly opposite to this is found in the Willmore Seismometer.

mass of the seismometer. The mass responds to this force as if the seismometer were subject to a ground acceleration $\frac{gi}{M}$.

A.2 Electromagnetic damping

Damping requires the application of a force to the pendulum which is proportional and opposite to the pendulum velocity. It may be obtained electromagnetically by shunting the coil with a suitable resistance. If the coil of resistance R_c is shunted by a resistor R_s then, neglecting the coil inductance, a current $\frac{gv}{R_s+R_c}$ will flow in the circuit and a force $\frac{g^2v}{R_s+R_c}$ will be applied to the suspended mass opposing its motion[2]. The potential difference across the shunt resistor may then be the seismometer output and is $\frac{gvR_s}{R_s+R_c}$

The electromagnetic damping constant is $\frac{g^2}{R_s+R_c}$ and is maximum if the coil is short circuited ($R_s = 0$). The maximum amount of electomagnetic damping which can be applied is proportional to the square of the transducer constant, and hence dependant on the characteristics of the transducer elements.

---

2. Note however, if the coil inductance is large enough, it can change this behaviour substantially.

Appendix B THE LAPLACE TRANSFORM AND TRANSFER FUNCTIONS

B.1 Laplace and inverse Laplace transforms

The Laplace transform of a function $f(t)$ of time is defined as

$$F(s) = \mathcal{L}[f(t)] = \int_0^\infty f(t) e^{-st} dt$$

where $s = \sigma + j\omega$ is the complex frequency.

The inverse Laplace transform of $F(s)$ is defined as

$$\mathcal{L}^{-1}[F(s)] = \frac{1}{2\pi j} \int_{-j\infty}^{j\infty} F(s) e^{st} ds = f(t)$$

In practice these integrals may be evaluated using complex variable theory or the results may simply be extracted from tables of Laplace transforms.

B.2 Transfer functions

The transfer function of a linear system is a function of the complex frequency s, and is defined to be the ratio of the exponential response to an exponential excitation. Thus, if a signal $v_i e^{st}$ is exciting a system of transfer function $G(s)$ the response will be $G(s) v_i e^{st} = v_o e^{st}$ and

$$G(s) = \frac{v_o e^{st}}{v_i e^{st}} = \frac{v_o}{v_i}$$

More generally, consider a signal $v_i(t)$ [$= 0$ for $t < 0$] which can be resolved into a series of exponential spectral terms by the Laplace transform:

$$v_i(t) = \frac{1}{2\pi j}\int_{-j\infty}^{j\infty} V_i(s)\, e^{st}\, ds$$

where $V_i(s) = \mathcal{L}[v_i(t)]$. The effect of each spectral term on the system response can be individually determined. The input spectral term at complex frequency s is $\frac{V_i(s)e^{st}ds}{2\pi j}$ and consequently, from the definition of the transfer function, the corresponding output term is $\frac{G(s)V_i(s)e^{st}ds}{2\pi j} = \frac{V_o(s)e^{st}ds}{2\pi j}$.

$$G(s) = \frac{V_o(s)}{V_i(s)} = \frac{\mathcal{L}[v_i(t)]}{\mathcal{L}[v_o(t)]}$$

is the general definition of the transfer function $G(s)$.

In words, the transfer function of a linear system is the ratio of the Laplace transform of a response to the Laplace transform of the excitation.

The transfer function of a system may be determined by taking the Laplace transform of the system differential equation.

A system with transfer function $G(s)$ is usually represented by a block in which the transfer function is printed. (Fig.B-1).

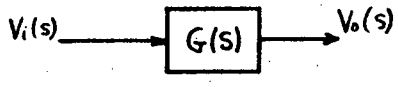

Fig.B-1 Block representation of a system with transfer function $G(s)$.

Appendix C FEEDBACK

C.1 The transfer function of feedback systems

Consider the system shown in the block diagram of Fig.C.1. $G(s)$ and $F(s)$ are transfer functions and $V_i(s)$, $V_o(s)$, and $E(s)$ are Laplace transforms of signals at the positions shown. The circular symbol is a subtractor, and indicates that part of the output ($F(s)V_o(s)$ in transform notation) is being added negatively to the input.

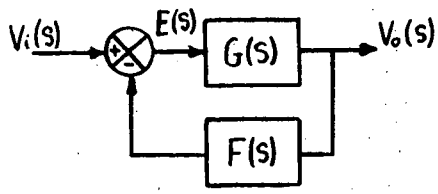

Fig.C-1 Block diagram of feedback system

Such a system is called a negative feedback system.

From Fig.C-1, $V_o(s) = E(s)G(s)$

and $$E(s) = V_i(s) - F(s)V_o(s)$$

Elimination of $E(s)$ gives $$H(s) = \frac{V_o(s)}{V_i(s)} = \frac{G(s)}{1+F(s)G(s)}$$

where $H(s)$ is the transfer function of the feedback system and is known as the closed loop transfer function. $F(s)G(s)$ is known as the open loop transfer function and also as the loop gain.

C.2 Stability of feedback systems

From a phsical point of view, if the feedback system experienced phase shifts at some value of the constant part of the loop gain such that the feedback signal would be added to rather than subtracted from the input, the system

would saturate or become unstable. Such possible phase shifts must be considered in the design of feedback systems.

From a mathematical point of view, the response of a general system with transfer function $H(s)$ to applied initial conditions is of the form $\sum_{k=1}^{n} C_k e^{s_k t}$ where the $s_k = \sigma_k + j\omega_k$ are the poles of $H(s)$, ie., $H(s_k) = \infty$, and n is the number of such poles. It is seen that associated with each pole is a characteristic exponential response $e^{s_k t}$. For the system to be stable, the characteristic exponentials must be damped: $\sigma_k < 0$. Hence the poles of $H(s)$ must lie in the left half s-plane.

If $H(s) = \frac{G(s)}{1+F(s)G(s)}$ for a feedback system, it is required that the roots of $1+F(s)G(s)=0$ lie in the left half s-plane.

This criterion is the basis of the various methods of stability analysis which are in use. The root locus method is discussed in Appendix D and other methods may be found in references 2 and 10.

C.3 System noise and feedback

A system with transfer function $G(s) = G_1(s)G_2(s)$ has a noise source $N(s)$ at the position shown in Fig.C-2. With zero input, the system output is $G_2(s)N(s)$. This output can be considered the result of a signal applied at the system input. This equivalent input noise is then $\frac{N(s)}{G_1(s)}$.

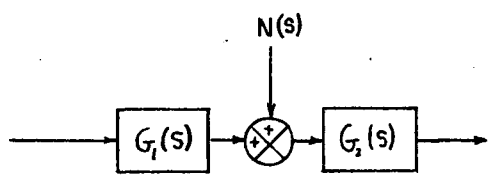

Fig.C-2 Block diagram of system with noise.

If a feedback path with transfer function $F(s)$ enclosed the system (Fig. C-3), we have, for zero input,

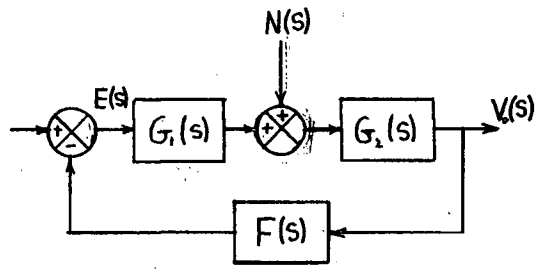

Fig. C-3 Block diagram of noisy system with feedback.

$$E(s) = -F(s)V_0(s)$$

and $$V_0(s) = G_2(s)N(s) + E(s)G(s)$$

giving $$V_0(s) = \frac{G_2(s)N(s)}{1 + F(s)G(s)}$$

which is the output noise due to the noise source $N(s)$.

The equivalent input noise is now

$$\frac{G_2(s)\,N(s)}{1 + F(s)G(s)} \cdot \frac{1 + F(s)\,G(s)}{G(s)} = \frac{N(s)}{G_1(s)}$$

which was the result for the system without feedback. Therefore, the equivalent input noise of a system is unaltered by the application of feedback, provided the feedback path contains no noise sources. It then follows that the signal to noise ratio of a system is the same before and after feedback is applied.

Appendix D ROOT LOCUS METHOD

D.1 Theory

The stability of a feedback system with transfer function $H(s) = \frac{G(s)}{1 + F(s)G(s)}$ depends on the position of the poles[1] of $H(s)$ in the complex frequency plane. (See Appendix C.2). The root locus method plots the positions of the roots of $1 + F(s)G(s)$ (poles of $H(s)$) on the s-plane with the loop gain as a parameter.

The equation $1 + F(s)G(s) = 0$ defining the roots reduces to two equations: $|F(s)G(s)| = 1$

$$\arg[F(s)G(s)] = \pi + 2\pi n \qquad n = 0, \pm 1, \pm 2, \ldots$$

The root locus is the locus of all points in the s-plane satisfying the phase condition, with the magnitude condition being used to determine the value of the loop gain at any point on the locus. As the loop gain increases from 0 to ∞ , the locus in general, originates at the poles of $F(s)G(s)$ (marked by $\times$), and terminates on the zeros[2] (marked by o), with the direction of gain increase being given by arrowheads on the locus. The value of the loop gain where the locus crosses into the right half of the s-plane ($\sigma = 0$) is the largest value for which the system will remain stable. This value will result in a steady undamped oscillation if linearity is maintained.

---

1. Poles of $X(s)$ are those s for which $X(s) = \infty$.
2. Zeros of $X(s)$ are those s for which $X(s) = 0$.

D.2 ζ_s and ω_s of second order systems from root locus diagrams

Consider a system with transfer function

$$\frac{E(s)}{\ddot{Y}(s)} = \frac{as}{s^2 + 2\zeta_s\omega_s s + \omega_s^2}$$

which may represent the acceleration sensitivity of an unloaded electromagnetic seismometer where $E(s)$ is the open circuit output voltage and $\ddot{Y}(s)$ is the input ground acceleration. In this case, $\omega_s = \sqrt{\frac{u}{M}}$, $\zeta_s = \frac{D}{2M\omega_s}$ and $a = \frac{g^2}{M}$. Also consider the application of negative acceleration feedback, for example, to the seismometer as shown in Fig.D-1. The open loop transfer function is

$$\frac{As^2}{s^2 + 2\zeta_s\omega_s s + \omega_s^2}$$

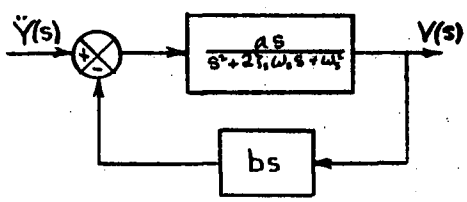

Fig.D-1. Block diagram of second order system with differentiating feedback loop.

with two zeros at the origin of the s-plane, and two poles at

$$s = -\zeta_s\omega_s \pm j\omega_s\sqrt{1-\zeta_s^2}$$

Pythagarus' theorem and elementary trigonometry show the length of a radius vector between the origin and one of these poles to be ω_s , and the angle between the radius vector and the negative real axis to be $\cos^{-1}\zeta_s$. The root locus for this feedback system is illustrated in Fig.D-2. As A increases, the poles of the feedback seismometer move along the circular arc comprising the locus from the poles of the open loop transfer function to the zeros. Since the feedback system is of second order,

its poles are determined by an equation of the form

$$s^2 + 2\zeta_s'\omega_s' s + \omega_s'^2 = 0$$

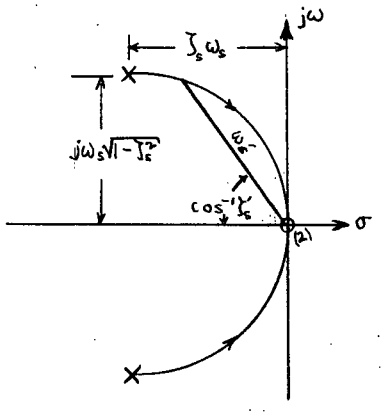

Fig.D-2 ζ_s' and ω_s' of second order system from root locus.

and are at

$$s = -\zeta_s'\omega_s' \pm j\omega_s'\sqrt{1-\zeta_s'^2}$$

ζ_s' and ω_s' are the damping ratio and angular natural frequency of the feedback seismometer and may be determined graphically as described above once the gain A and hence the positions of the poles on the locus are specified (Fig.D-2). For $A = 0$, the poles of the feedback seismometer are coincident with those of the seismometer before feedback was applied and $\omega_s' = \omega_s$ and $\zeta_s' = \zeta_s$.

Root locus diagrams can thus be used to study the effect of various types of feedback on the natural frequency and damping ratio of the seismometer.

Appendix E OPERATIONAL AMPLIFIERS

E.1 Transfer function of operational amplifiers

An operational amplifier is a high gain dc amplifier. When a vacuum tube operational amplifier is enclosed by a feedback path as in Fig.E-1, the input to the amplifier becomes a virtual ground. Since the currents flowing into this junction must sum to zero, in transform notation, $\frac{V_o}{Z_f} + \frac{V_i}{Z_i} = 0$ and $\frac{V_o(s)}{V_i(s)} = \frac{Z_f(s)}{Z_i(s)}$ is the transfer function of the system.

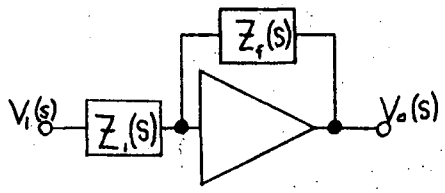

Fig.E-1 Operational amplifier.

If Z_i and Z_f are resistances R_i and R_f, then

$$\frac{V_o(s)}{V_i(s)} = -\frac{R_f}{R_i}$$

which is the Laplace transform of $v_o(t) = -\frac{R_f}{R_i} v_i(t)$. An operational amplifier operated in this manner is a phase inverter and multiplier.

If Z_i and Z_f are respectively a resistance and a capacitance, then, for no initial charge on the capacitor,

$$\frac{V_o(s)}{V_i(s)} = -\frac{1}{R_i C_f s}$$

which is the Laplace transform of $v_o(t) = -\frac{1}{R_i C_f}\int v_i(t)\,dt$, and the system performs an integration with a gain of $\frac{1}{R_i C_f}$.

Similarily, if Z_i is a capacitance and Z_f a resistance then $\frac{V_o(s)}{V_i(s)} = -R_f C_i s$ and $v_o(t) = -R_f C_i \frac{dv_i(t)}{dt}$.

Several signals can be combined as shown in Fig.E-2

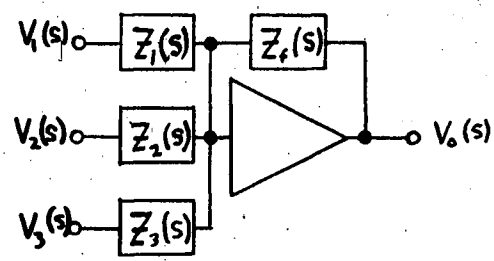

Fig.E-2 Operational amplifier with several input signals.

with $$V_o(s) = -\frac{Z_f}{Z_1} V_1(s) - \frac{Z_f}{Z_2} V_2(s) - \frac{Z_f}{Z_3} V_3(s)$$

While transistor operational amplifiers operate in a different manner, the result is the same.

E.2 Block symbols of operational amplifiers

Three standard block symbols which appear in the thesis are illustrated in Fig.E-3.

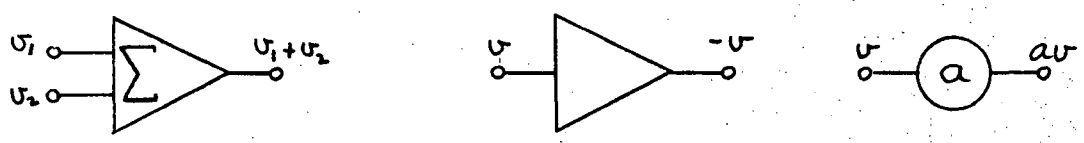

a) summing amplifier b) phase inverter c) multiplication by a constant

Fig.E-3 Series of standard block symbols.